Departments of Mathematics, Physics and DACSO

MASTER THESIS

Modelling for Science and Engineering

Comparison between two Planetary Boundary Layer schemes in the Weather Research and Forecasting model coupled with Chemical transport (WRF-Chem)

Oriol Teixidó Garcia

October 2020

Tutor **Dr. Alba Badia Moragas**

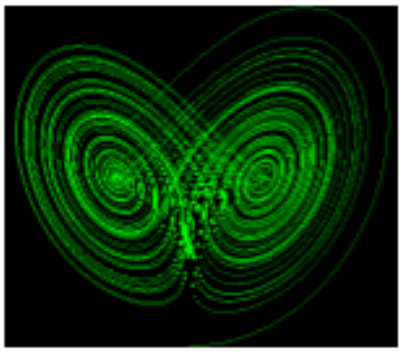

Universitat Autònoma de Barcelona - 2 October 2020

Contents

List of Figures

List of Tables

Abstract

Currently, around 54% of the world's population is living in urban areas and this number is projected to increase by 66% by 2050. Air pollution (NO_2, CO, PM_{10}, $PM_{2.5}$ and VOCs) mainly from transport mobility, heating and cooling in cities, is considered the single largest environmental health hazard in Europe and is responsible for 467,000 premature deaths per year. Air quality has been identified as a major threat to human health and the ecosystem, especially in urban areas, where exposure to air pollution is the highest. Urban air quality modeling has been the focus of considerable development during recent decades, driven by this concern. Numerous air quality models have been developed by different research groups and are being used for designing emission control policies. The Weather Research and Forecasting model (WRF) coupled with chemical transport (WRF-Chem) developed by NCAR (http://www.wrf-model.org/index.php) with multi-layer canopy model (BEP+BEM) offers the ability to simulate the air quality at urban scale. The main objective of this thesis is to perform an evaluation of the outputs of the WRF-Chem model (relevant air pollutants, which are the carbon monoxide (CO), the nitrogen monoxide (NO), the nitrogen dioxide (NO_2), the ozone (O_3) and the particulate matter with a diameter between 10 and 2.5 μm (PM_{10}), and meteorological data) in order to determine and quantify the model's performance capabilities and weaknesses. Specifically, we will examine and contrast two different Planetary Boundary Layer schemes, MYJ and BouLac, to model the urban atmospheric chemistry over the city and the Metropolitan Area of Barcelona. The aforementioned comparison is going to be performed between the two schemes and with real data, using the data of the "Xarxa de vigilància de la contaminació atmosfèrica". The period that we use for the simulation is the month of July of 2016. To do such work, we will need to make use of a supercomputer, Picasso, from the Red Española de Supercomputación (RES) situated in the University of Malaga (UMA). Finally, we will see that the best PBL scheme for modelling urban areas depends on the air pollutant and on the location of the stations. The scheme that better predicts the reality is the MYJ, although the BouLac present better results for the modeling of nitrogen oxides inside the Barcelona city. This study will be used in the URBAG project (https://urbag.eu/).

1 Introduction

The atmospheric pollution is a dangerous and increasing issue for living beings. The fact that more than half of the global population is living in urban areas causes that its air quality is being more damaged than ever. Only in the city of Barcelona, the air exceeds the levels established from the World Health Organisation (WHO) on six pollutants: the nitrogen dioxide (NO_2), the particulate matter with a diameter between 10 and 2.5 μm (PM_{10}), the particulate matter that has a diameter less than 2,5 μm ($PM_{2.5}$), the benzene, the benzene(a)pyrene and the levels of ozone (O_3). According to the study "Air quality evaluation in Barcelona in 2016" realized by the Public Health Agency of Barcelona (ASPB, for its acronym in Catalan), the 68% of the population is exposed to annual levels of NO_2 greater than the fixed from the WHO, and respect to the particulate matter is of the 95%. It is calculated that the reduction of these particles would avoid near of 650 deads per year in the city and 3500 within the metropolitan area. Is for that reason that we need reliable instruments for the simulation and prediction of the air contamination levels: the atmospheric models.

An atmospheric model is a mathematical model constructed around the full set of primitive dynamical equations which governs atmospheric motions to simulate the interactions of the important drivers of climate. It can supplement these equations with parameterizations for turbulent diffusion, radiation, moist processes (clouds and precipitation), heat exchange, soil, vegetation, surface water, the kinematic effects of terrain, and convection. Most atmospheric models are numerical, i.e. they discretize equations of motion. They can predict microscale phenomena such as tornadoes and boundary layer eddies, sub-microscale turbulent flow over buildings, as well as synoptic (anomalies in sea level pressure) and global flows. The horizontal domain of a model can be either global, covering the entire Earth, or regional (limited-area), covering only part of the Earth. As we want to study the urban climatology, using as city test the the Metropolitan Area of Barcelona, related to the air pollution, we use the regional model called Weather Research and Forecasting (WRF) model with Chemical transport (WRF-Chem) coupled with the urban canopy model BEP+BEM. This is an online model described in the section 3.1.

If we talk about atmospherical modeling, we must mention the layer where all the main atmospherical processes occur and which is directly coupled with the earth's surface. This layer is the Planetary Boundary Layer (PBL). The modelers make effords to build and improve schemes for modeling and representing the processes of that layer to suit them with the conditions of the kind of region which they want to simulate. Indeed, there are different handicaps in the atmospherical modeling over the urban areas than modeling over natural regions or at global scales: these are the morphology of the city and the impact of the anthropogenic heat (AH). An intensive effort has been carried out for the community mesoscale WRF model [5] to improve its skills in urban areas and to be able to assess environmental problems such as the urban heat islands (UHI) and urban air pollution. Therefore, revised PBL schemes capable of being coupled with urban models taking account that facts are necessary. Bougeault-Lacarrere (BouLac) scheme [4] and the Mellor-Yamada-Janjic (MYJ) [15] are the two PBL schemes that can be coupled with an urban model to treat the urban scenario and the ones we use in this work.

The story of climate modeling, using numerical methods, begins with Lewis Fry Richardson, an English mathematician and meteorologist, when he publishes a book entitled "Weather Prediction by Numerical Process". The book describes his idea for a new way to forecast the weather using differential equations and viewing the atmosphere as a network of gridded cells. But when he applied his own method, it took him six weeks doing calculations by hand just to produce an eight-hour forecast. He imagined a stadium full of "computers" (64,000 human calculators) all working together to speed up the process. But without mechanical computers, his attempts failed. Fortunately for Lewis F. Richardson, humanity advanced to such a level that we invented not only ordinary computers, but we also invented the supercomputers! A supercomputer is a computer with a high level of performance as compared to a general-purpose computer. The performance of a supercomputer is commonly measured in floating-point operations per second (FLOPS) instead of million instructions per second (MIPS). Since 2017, there are supercomputers that can perform over 1017 FLOPS (a hundred quadrillion FLOPS, 100 petaFLOPS or 100 PFLOPS). In order to compile the WRF-Chem model, we have access to one supercomputer of the "Red Española de Supercomputación" (RES), the Picasso supercomputer, located at the University of Malaga (UMA).

In this thesis, we are going to decide which PBL scheme, between BouLac and MYJ, better predicts and simulates the level of contamination in urban regions. In particular, we will use Barcelona and the metropolitan area as the test city. So as to do that decision, we have for our use the data of the concentration of 5 pollutants in a set of stations (8 stations for the carbon monoxide (CO), 22 for the nitrogen monoxide (NO), 22 for the nitrogen dioxide (NO_2), 13 for the ozone (O_3) and 11 for the PM_{10}) located around Barcelona and its metropolitan area. This data is provided by the "Xarxa de vigilància de la contaminació atmosfèrica" and give us the observed concentration at the ground level for each pollutant in the station. In the process of arriving to the final decision, we will have to preprocess the data for the model, compile and run it to obtain the concentration of each air pollutant through all Catalonia. After that, we must select the data in the coordinates where the stations are located and compare that data with the observed one. We have for every station the information of the type of the urban region (if it is in the urban, peri-urban or in a rural zone), and we will find correlations with that data. Where we also find correlation, between the best scheme and the stations, is if the station is inside or outside of Barcelona city.

The work is splited in four parts. In the section two, we give an explanation of the fundamental theoretical aspects needed to understand the results and to make a rigorous discusion. In there, we comment the physical and chemical aspects within the PBL, its behavior, the pollutants and the emissions of them. In the following section, the third, we describe the tools used in this work, as well as we give a brief description and the set-up of the model. The fourth is reserved for an explanation of how we handle with experimental and predicted data. Finaly, in the section five, we expose the results and argue the final decision.

2 Theoretical framework

In this thesis, we are going to use the ground-level concentration of pollutants of the group of atmospheric stations that we have mentioned, in order to achieve our goal of deciding which PBL scheme predicts better the level of pullution. To do such a study, we need to understand the physical and chemical behavior within the layer that affects the most to the air pollution and to human life, the PBL. After that, we will invest a part of this section to make a brief description of the pollutants that we will use in our analyzis, as well as their evolution within the PBL, the reactions in which they are involved and the healthy effects. Finally, an explanation about the type of emissions and its influence will be exposed.

2.1 The PBL

Through the PBL, rapid exchanges of momentum, heat, moisture, natural, and anthropogenic chemical constituents take place between the free atmosphere and surface characteristics, including soil, the vegetation of different varieties, water, ice, and snow. In this layer, physical quantities such as flow velocity, temperature, and moisture display rapid fluctuations (turbulence) and the vertical mixing is strong. Above the PBL is the "free atmosphere", where the wind is approximately geostrophic (parallel to the isobars), while within the PBL the wind is affected by surface drag* and turns across the isobars.

A fundamental variable of the PBL is its top height (PBLH) that determines many tropospheric processes critical to air pollution, such as aerosol distributions, convection activity, and cloud and fog formation [17]. The PBLH has been used as a key length scale in weather, climate, and air quality models to determine turbulence mixing, vertical diffusion, convective transport, cloud/aerosol entrainment, and atmospheric pollutant deposition. The PBLH variability is dominated by its strong diurnal cycle [25]. It is typically shallow (<500 m) at night, as the surface layer becomes stable because of infrared radiative cooling; whereas it grows deep (penetrating a few kilometers) in daytime when solar heating causes convective unstable conditions. The PBLH, however, is not directly observed by routine meteorological measurements. It is often diagnosed from vertical profiles of temperature, humidity, and wind. These profiles are conventionally measured with radiosondes. Even if we do not have the experimental value of the PBLH, we can use the value that the model gives us to make predictions of the temporal behavior of the pollutant concentrations. For example, from the diurnal cycle, we can intuit that the pollutant concentration has to be higher at night (when the PBLH is shorter) and lower in the day (when the PBLH is taller). We can see the PBL cycle in figure 1.

*In fluid dynamics, drag (sometimes called air resistance, a type of friction, or fluid resistance, another type of friction or fluid friction) is a force acting opposed to the relative motion of any object moving with respect to a surrounding fluid. This can exist between two fluid layers (or surfaces) or a fluid and a solid surface. Unlike other resistive forces, such as dry friction, which are nearly independent of velocity, drag forces depend on velocity.

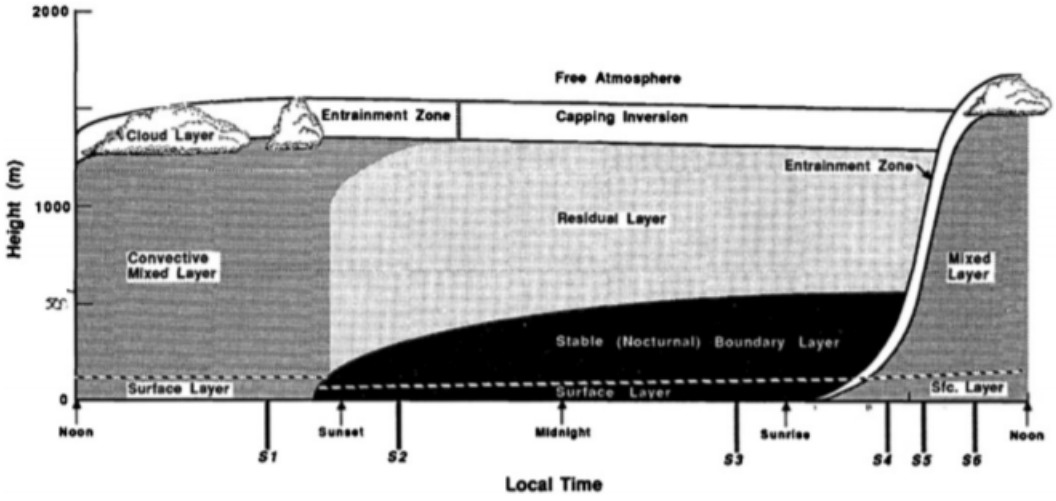

Figure 1: Constituents of the PBL and their evolution through the diurnal and nocturnal cycle. Image extracted from: An introduction to boundary layer meteorology "R. B. Stull." .

The PBL structure during a diurnal cycle can be classified into three major regimes [25]: convective boundary layer (CBL), stable boundary layer (SBL), and residual layer (RL). The CBL usually occurs in the daytime and is driven by convective thermals generated as a result of heat transfer from a warm ground or radiative cooling from a cloud top. Strong turbulence mixing causes nearly uniform vertical distributions of potential temperature and constituents within the CBL. Conversely, the SBL forms often in the nighttime because of radiative cooling of the ground or sometimes as warm air is advected over a colder surface. Both conditions create a boundary layer of air that is warmer than the underlying surface, and turbulence mixing is largely suppressed in the SBL. In the evening or morning transition, the RL is disconnected from the ground by the underlying SBL while maintaining the atmospheric state of the former CBL. Thus, the RL is not affected by turbulent transport from the surface but allows turbulence to decay homogenously in all directions [17].

2.2 Pollutants and their origin

The physical nature and the composition of the atmospheric chemical pollutants are highly variated. Not only for their natural or anthropogenic origin, but also the pollutants can be classified in primary and secondary. The primaries are substances poured directly into the atmosphere, it is found among them the aerosols or particular matter, the sulfur dioxides, the nitrogen oxides, the carbon monoxide and the hydrocarbons. The secondary pollutants are substances that are produced as a consequence of the transformations, chemical and photochemical reactions, that the primary pollutants suffer within the atmosphere [2]. We recall that the air constituents that we study in this work are the CO, NO, NO_2, O_3 and PM_{10}.

2.2.1 Pollutants

Carbon monoxide (CO)

CO is one of the most important trace gases in the troposphere, exerting a significant influence upon the concentration of oxidants such as OH and O_3 [28]. The main sources of CO in the troposphere are the photochemical production from the oxidation of hydrocarbons (including methane) and direct emissions, mainly fossil fuel combustion, biomass burning and biogenic emissions. CO main loss is by reaction with OH, which occurs primarily in the tropics, but also in the extratropics [3].

Breathing CO can cause headache, dizziness, vomiting, and nausea. If CO levels are high enough, one may become unconscious or die. Exposure to moderate and high levels of CO over long periods of time has also been linked with an increased risk of heart disease. People who survive severe CO poisoning may suffer long-term health problems [12].

Nitrogen compounds

The NO_x (= NO_2 + NO) family is one of the key players in the chemical processes related to O_3 in the troposphere, causing photochemical smog and contributing to acid rain during pollution episodes. As a consequence of its relatively short lifetime (a few hours within the PBL and up to a few days in the upper troposphere; [26, 27]), it is generally restricted to emission sources, both natural and anthropogenic (mainly fossil fuel combustion). As a result, NO_x concentration is more sensitive to errors in emissions than other pollutants [3].

Long-term exposure to low levels of nitrogen oxides can cause asthma and respiratory infections, whereas the health effects from very high levels of nitrogen oxides can include death, genetic mutations, harm to a developing fetus, decreased female fertility, swelling of the throat and rapid pulse [20].

Ozone (O_3)

The ozone presence is distributed for the different layers and heights of the atmosphere and have different effects depending on the altitude. Above the stratosphere, the ozone is created by means of ultraviolet rays from the sun colliding to oxygen molecules. This photochemical reaction mainly take place between 15 and 35 km of heigh. There, ozone absorbs the ultraviolate (UV) light and it is beneficial for living beings. Penetrating in the stratosphere (20 km of height), the ozone contributes to the planet-warming acting as a greenhouse gas. The tropospheric, or ground level ozone, is not emitted directly into the air, but is created by chemical reactions between oxides of nitrogen (NO_x) and volatile organic compounds (VOC) and by stratospheric intrusions. The ozone creation takes place when pollutants emitted by cars, power plants, industrial boilers, refineries, chemical plants, and other sources chemically react in the presence of sunlight (we can see the ground-level creation of ozone ilustrated in figure 2).

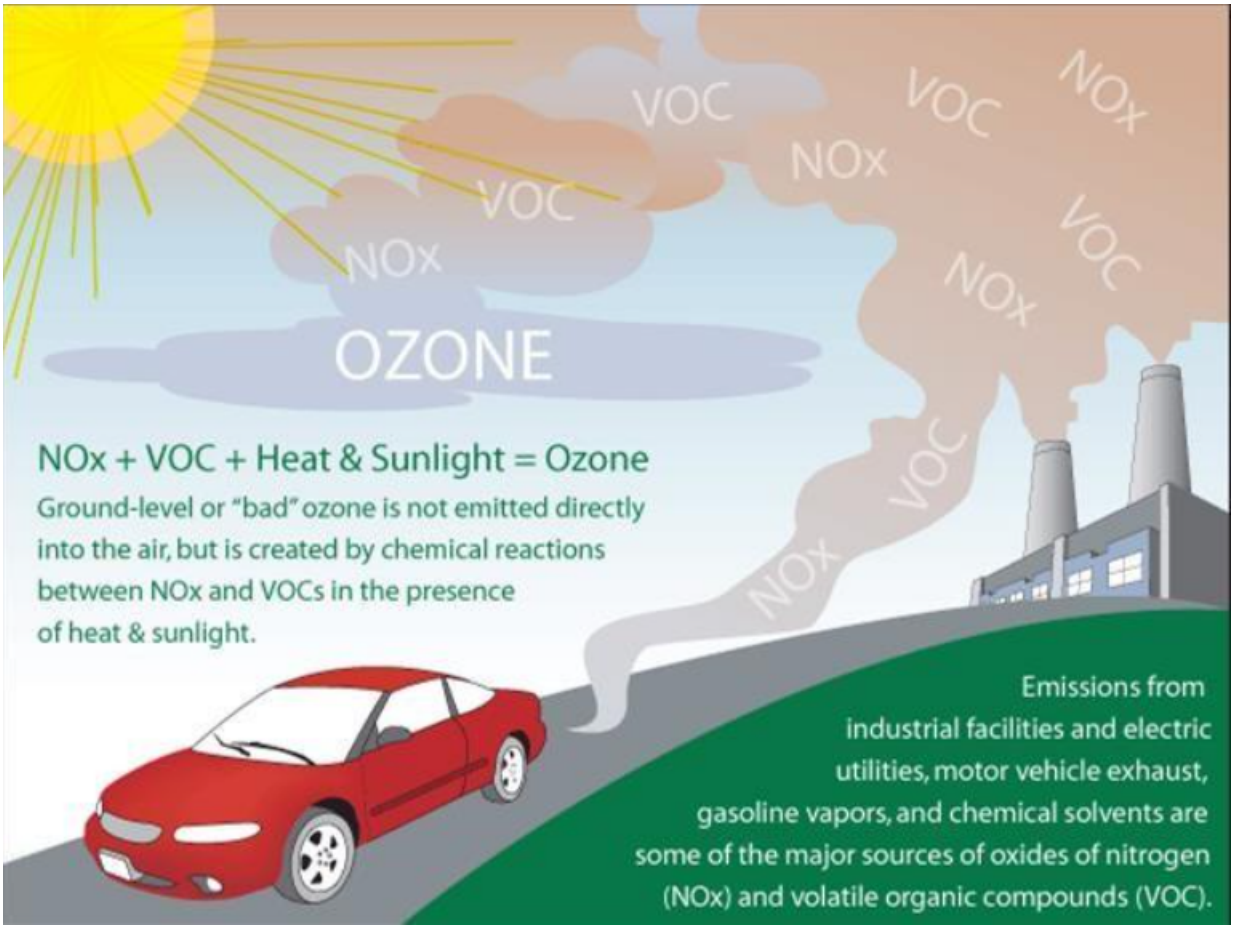

Figure 2: Illustration of the ozone creation by means of photochemical reactions between other air pollutants. Image source https://www.epa.gov/ground-level-ozone-pollution/ground-level-ozone-basics

From the explanation of above, we can note down that, as ozone is created by means of photochemical reactions, the presence of ozone in the atmosphere increases during the light-time period of the day (contrary to the concentration of the other pollutants). Furthermore, we have to take into account that the ozone affects to the concentration of other atmospheric components [22, 9].

The effects of ozone in a short term exposure can cause chest pain, throat irritation, coughing, and breathing difficulty; while long term exposure can lead to lung damage, asthma, and premature death in people with lung or heart disease [21]. The ozone at the groundlevel causes toxic fog.

Particulate matter (PM_{10})

The term "particulate matter" (also called particle pollution) is for a mixture of solid particles and liquid droplets found in the air. Some particles, such as dust, dirt, soot, or smoke, are large or dark enough to be seen with the naked eye. These particles come in many sizes and

shapes and can be made up of hundreds of different chemicals. Some are emitted directly from a source, such as construction sites, unpaved roads, fields, smokestacks or fires. Most particles are formed in the atmosphere as a result of complex reactions of chemicals such as sulfur dioxide and nitrogen oxides, which are pollutants emitted from power plants, industries and automobiles.

Exposure to such particles can affect both your lungs and your heart. Numerous scientific studies have linked particle pollution exposure to a variety of problems, including premature death in people with heart or lung disease, nonfatal heart attacks, irregular heartbeat, aggravated asthma, decreased lung function and increased respiratory symptoms, such as irritation of the airways, coughing or difficulty breathing.

2.2.2 Emissions

The air pollutant emissions cause air pollution, however, reductions in emissions do not always automatically result in similar cuts in concentrations. There are complex links between air pollutant emissions and air quality. These include emission heights, chemical transformations, reactions to sunlight, additional natural and hemispheric contributions and the impact of weather and topography. Although, significant cuts in emissions are essential for improving air quality. Air pollutants are emitted from a range of both man-made and natural sources including burning of fossil fuels in electricity generation, transport, industry and households; industrial processes and solvent use, for example in the chemical and mining industries; agriculture; waste treatment; natural sources, including volcanic eruptions, windblown dust, sea-salt spray and emissions of volatile organic compounds from plants [1]. We can see the emissors in figure 3.

3 Methodology

The tools used in this work has been the Weather Research and forecasting model with the chemical transport (WRF-Chem), the supercomputer Picasso, and the programming lenguage Python to analyze and present the results.

3.1 The WRF-Chem Model

The WRF Model is a next-generation mesoscale numerical weather prediction system designed for both atmospheric research and operational forecasting applications. It features two dynamical cores, a data assimilation system, and a software architecture supporting parallel computation and system extensibility. The model serves a wide range of meteorological applications across scales from tens of meters to thousands of kilometers. The effort to develop WRF began in the latter 1990's and was a collaborative partnership of the National Center for Atmospheric Research (NCAR), the National Oceanic and Atmospheric Administration (represented by the National Centers for Environmental Prediction (NCEP) and the Earth System Research Laboratory), the U.S. Air Force, the Naval Research Laboratory, the University of Oklahoma, and the Federal Aviation Administration (FAA).

Figure 3: Emissors of air pollutants. Source: EEA Signals 2013

For researchers, WRF can produce simulations based on actual atmospheric conditions (i.e., from observations and analyses) or idealized conditions. WRF offers operational forecasting a flexible and computationally-efficient platform, while reflecting recent advances in physics, numerics, and data assimilation contributed by developers from the expansive research community. WRF is currently in operational use at NCEP and other national meteorological centers as well as in real-time forecasting configurations at laboratories, universities, and companies.WRF has a large worldwide community of registered users (a cumulative total of over 48,000 in over 160 countries), and NCAR provides regular workshops and tutorials on it.

WRF-Chem is the Weather Research and Forecasting (WRF) model coupled with Chemistry. The model simulates the emission, transport, mixing, and chemical transformation of trace gases and aerosols simultaneously with the meteorology. The model is used for investigation of regional-scale air quality, field program analyzis, and cloud-scale interactions between clouds and chemistry.

Usage:

Before starting to run the model, we need to preprocess the data using the WRF Preprocessing System (WPS). The WPS is a set of three programs whose collective role is to prepare input to the real.exe program for real-data simulations. Each of the programs performs one stage of the preparation: geogrid defines model domains and interpolates static geographical data to the grids; ungrib extracts meteorological fields from GRIBformatted files; and metgrid horizontally interpolates the meteorological fields extracted by ungrib to the model grids defined by geogrid. The simulation domain is defined using information specified by the user in the namelist record of the WPS namelist file, namelist.wps [7].

The data flow between the programs of the WPS is shown in the figure 4. Each of the WPS programs reads parameters from a common namelist file, as shown in the figure. This namelist file has separate namelist records for each of the programs and a shared namelist record, which defines parameters that are used by more than one WPS program. With the data preprocessed, we can compile and run the WRF-Chem model.

The WRF model has two large classes of simulations that it is able to generate: those with an ideal initialization and those utilizing real data. The WRF model itself is not altered by choosing one initialization over another, but the WRF pre-processors are specifically built based upon a user's selection. In our case, we have used the real class. The real-data WRF cases are those that have the input data to the real.exe program provided by the WRF Preprocessing System (WPS). The data from the WPS originally came from a previously run, external analyzis or forecast model.

3.1.1 Urban Canopy model

As we have said, in this project, we lead our attention to the urban areas. In this context, it exist an urban canopy model with the finality of model the physical processes and energy exchanges

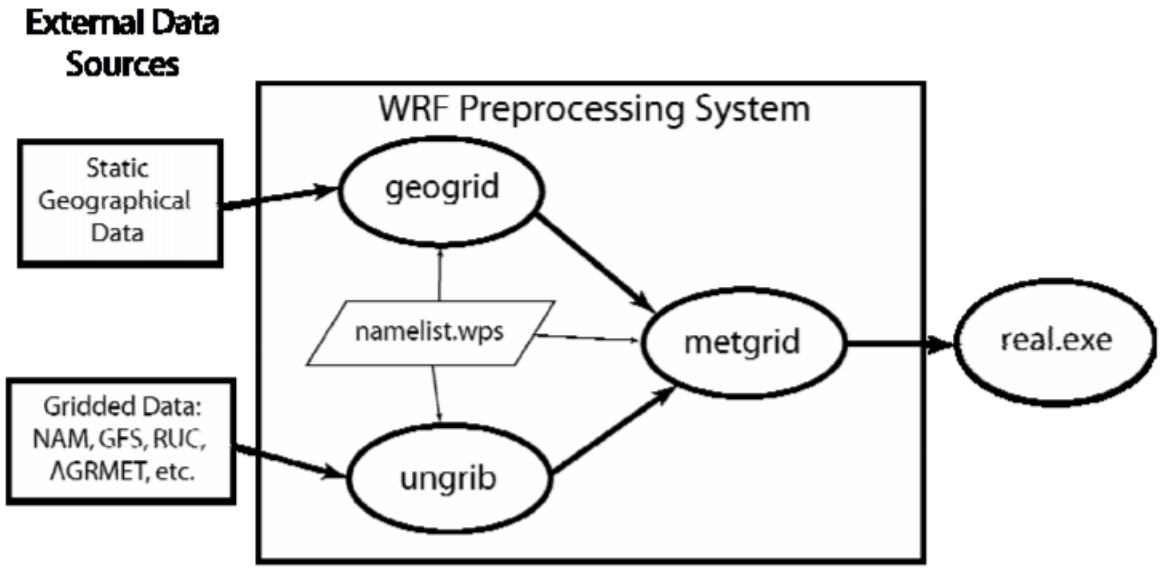

Figure 4: The flow of the data between the WPS programs.

within the urban regions. The urban parameterization was developed by [18], and it is a multi-layer urban canopy scheme called BEP (which stands for building effect parameterization; it had included in the WRF V3.1 release since 2009). BEP recognizes the three-dimensional nature of urban surfaces and the fact that buildings vertically distribute sources and sinks of heat and momentum through the whole urban canopy layer. It takes into account the effects of the vertical (walls) and horizontal (streets and roofs) surfaces on momentum, turbulent kinetic energy, and potential temperature. The wall and road radiation consider shadowing, reflection, and trapping of shortwave and longwave radiation in the urban canyons. The urban canopy scheme that we use is the result of the coupling between BEP and a simple building energy model (BEM). BEM accounts for the 1) diffusion of heat through the walls, roofs, and floors; 2) radiation exchanged through windows; 3) longwave radiation exchanged between indoor surfaces; 4) generation of heat due to occupants and equipments; and 5) air conditioning, ventilation, and heating. The BEP+BEM parameterization takes into account the exchanges of energy between the interior of the buildings and the outdoor atmosphere. Consequently, the impact of air conditioning systems (AC) and their energy consumption is estimated. The new BEP+BEM scheme had been included in WRF V3.2 release on April 2010.

3.1.2 Description of the PBL Schemes

PBL schemes are used to parameterize the unresolved turbulent vertical fluxes of heat, momentum, and constituents such as moisture within the planetary boundary layer and throughout the atmosphere. A closure scheme is needed to obtain turbulent fluxes from mean quantities [13]. One type of closure scheme estimates the turbulent fluxes at each point in model grids from the mean atmospheric variables and/or their gradients at that point. This is called local

closure. The assumption that fluxes depend solely on local values and gradients of basic model variables is least valid under convective conditions when turbulent fluxes are dominated by large eddies that transport fluid longer distances [14]. Both schemes that we use in this work are local.

Comparison between the PBL schemes

In WRF model, PBL schemes represent the turbulent subgrid-scale processes computing boundary layer fluxes of heat, moisture, and momentum in the lowest atmosphere, along to resolve vertical diffusion due to turbulence for the entire vertical column. There are two available PBL schemes that can be coupled with the BEP+BEM urban canopy model; the BouLac and the MYJ. Both schemes are one-and-a-half order prognostic turbulent kinetic energy (TKE)[19] schemes with local vertical mixing, although BouLac scheme has a non-local counter gradient term for convective conditions. Local closure schemes only allow vertical mixing between adjacent vertical layers unlike non-local closure schemes, which allow vertical diffusion between non-adjacent layers. Local schemes work well representing stable boundary layer situations while non-local schemes are better for unstable turbulent boundary layers. MYJ is more widely used than BouLac and is a modified version of the old ETA scheme from the "Fifth-Generation Penn State/NCAR Mesoscale Model" (MM5) model. BouLac scheme is less used, but it has been designed for use it with the BEP multi-layer and has been tested most extensively with BEP and BEP+BEM. Both schemes determine the PBL height from the TKE prognostic variable, at the height where the TKE decreases below a certain value, being 0.2 m2s-2for the MYJ scheme and 0.005 m2s-2for the BouLac scheme. For this reason, we can expect that the BouLac scheme predicts higher PBL schemes than the MYJ scheme. This fact affects to the concentration of the atmospherical components since they are more "tighty" when using the MYJ scheme. Therefore, we could expect higher concentrations with the MYJ scheme.

3.2 Model set-up

Two air quality simulations with a different PBL scheme are performed and compared with the observations. The period that we simulate is the month of july of 2016 and the domain is all Catalonia 5.

The model is set up with a horizontal resolution of 3 km×3km and 45 vertical layers up to 100 hPa. The meteorological initial and lateral boundary conditions were determined using the Final analyzis (FNL) of the NCEP global model data. Chemical initial and boundary conditions are from the global atmospheric model MOZART-4 global chemical model [6].

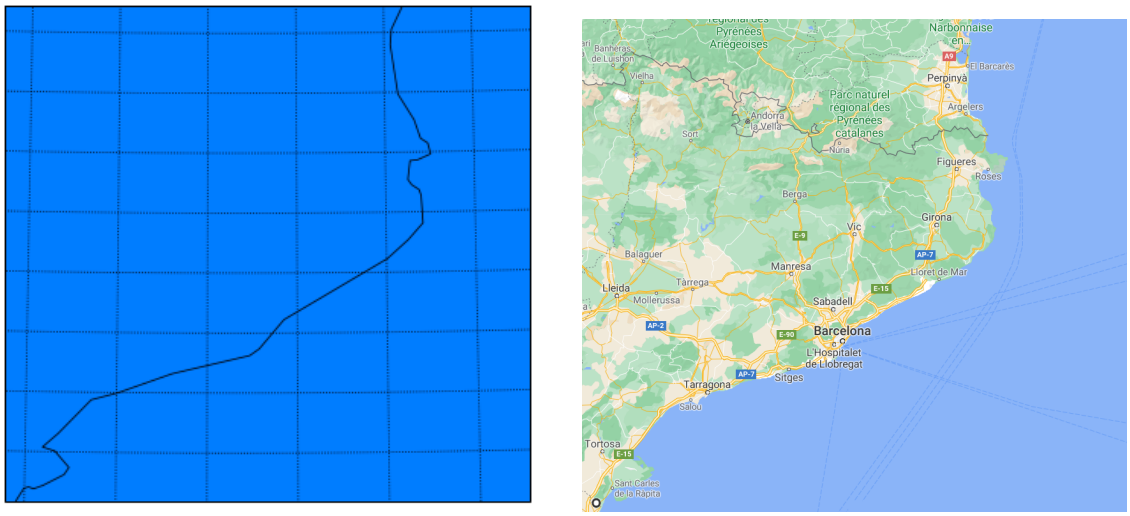

(a) Countorn of the region that we have modeled ploted with python.

(b) The corresponding geographical map of our domain.

Figure 5: Domain of the region that we model.

Here we used the multi-layer layer scheme, the Building Effect Parameterization (BEP) coupled with the Building Energy Model (BEP+BEM, [23]) to take into account the energy consumption of buildings and anthropogenic head generated by air conditioning systems. As well as, the Local Climate Zones (LCZ) classification [24] is used where specific values for each LCZ for thermal, radiative and geometric parameters of the buildings and ground are used by the BEP+BEM scheme to compute the heat and momentum fluxes in the urban areas.

Another tool that we are using for our study is the the High-Elective Resolution Modelling Emission System version 3 for Global and Regional domains (HERMESv3_GR, [11]). HERMESv3_GR is a stand-alone multiscale atmospheric emission processing system that processes and estimates emissions for global and regional air quality modelling. The HERMES preprocessor tool was used in order to create the anthropogenic emissions files from the CAMS-REG_Apv2.2.1 database [16]. Biogenic emissions are computed online from the Model of Emissions of Gases and Aerosols fromNature v2 (MEGAN; [10]).

We have in the table 1 a summary of the model details and the configuration of the experiment.

Model	
Model and version	WRF-Chem v4.1 [8]
Resolution and initial conditions	
Horizontal resolution	3km x 3km
Vertical Layers	46
Top of the atmosphere	100hPa
Chemical initial and boundary conditions	MOZART-4 global %ref
Physics	
Urban scheme	BEP+BEM and LCZ
PBL scheme	Bougeault and Lacarrere (BouLac) or Mellor-Yamada-Janjic (MYJ)
Chemistry	
Chemical mechanism	Regional Acid Deposition Model (RADM2) and MADE/SORGAM aerosols
Emission inventories	
Biogenic emissions	MEGAN
Anthropogenic emissions	global HERMESv3

Table 1: Model details and experiment configuration.

3.3 Picasso Supercomputer

The University of Málaga (UMA) has a strong tradition on Supercomputing that goes back to the decade of the 90's where parallel computers were mainly used for research on parallelization of computation-intensive applications.

It was on 1997 when the first supercomputer was installed, dedicated exclusively to the execution of scientific applications by the UMA researchers. It was called "Picasso", a SGI Origin 2000.

Nowadays the supercomputing facilities that gives support to research activity is composed by a set of HP supercomputers accessible to the entire scientific community. Supercomputing managers and administrators are also giving advise to users on computation problems or on data processing, as well as on the optimal use of the available tools at the hardware and software levels.

Picasso belongs to the Red Española de Supercomputación (RES). The RES is an infrastructure distributed that consist in the interconnection of 12 supercomputers with the aim of ofering computational resources of high performance in the cientific comunity. The RES is coordinated by the Barcelona Supercomputing Center (BSC). RES is a cientific and singular technical infrastructure (ICTS).

4 Postprocessing the data

Before starting with the results, we want to give an explanation of the tables and the graphics that we are going to show in order to focus all the attention in the results in the next section. In that way, we follow with a guideline of how the results have been organised:

1. First of all, we begin with a vertical profile for all the air pollutants concentration in the city of Barcelona, with who we will observe the first differences between the PBL schemes. In the vertical profile, we will see that the air pollutant concentration changes its regularity depending on if we are studying the weekdays or the weekends, although only the prediction of PM10 is really affected by that fact.
2. In the next step, we split up the results by the five air pollutants. In this, we are going to show a summary table with the statistical errors for each station. As we have too many stations for analysing them one by one, we will compare the best and the worst prediction for each air pollutant.
3. Finally, we will present a map of Barcelona and the metropolitan area, placing the stations on the map and showing the better scheme for them. In that way, we want to study possible correlations between the best predictions and the type of the station.

We have simulated the entire month of July of 2016. However, we use the data of the last two weeks because the first two weeks are the spin-up for the chemistry.

4.1 Vertical profile

In the vertical profile, we are going to gather the simulated data of Barcelona city. We will compute the mean of the pollutant concentration of a square of 18km×6km centered in the Eixample (latitude: 41.5833, longitude: 2.2333) for each atmospherical layer. In this graphic, we will show a colormap with the atmospherical height in the vertical axis and the time in the horizontal. We are using for this graphic the outputs of the model from the Saturday 16^{th} to the Friday 29^{th} of July. To be more precise and reduce the effects of having unusual days related with the emissions, we compute a mean for the same days of the week (a mean with the outputs of the Saturday 16^{th} and the Saturday 23^{th}, another for the Sundays, Mondays and the same for the rest days of the week). In the vertical axe, we are going to cut the data in the half of the height of the PBLH of the MYJ scheme, since it is the shortest and we want to study the ground-level pollution. Using the same top height for both schemes, we will be able to compare the two vertical profiles in the same contest. Moreover, we add a second vertical axis to the right with the mean of the concentration for all the vertical column for each hour. With that graphic, we can compare the amount of concentration predicted for each scheme, as well as observe the temporal behavior of the predicted pollution.

4.2 The hourly mean of concentration

For the comparison among the model outputs and the real data, we will use an hourly mean of 24 hours, separating the data between the weekdays and the weekends. For the weekdays, we use the data of the days from the 18^{th} to the 22^{nd} added to the data from the 25^{th} to the 29^{th}, whereas for the weekends we use the results of the days from the 16^{th} to the 17^{th} and from the

23^{rd} to the 24^{th}.

We compute this hourly mean with the days within the two periods (weekdays or weekends), taking the concentration of the first day at 00:00 a.m., the concentration for the second day at 00:00 a.m.,... until the last day and we compute the average. One time we have the average for the first hour, we compute the average of the concentration of all the days at the next hour, and the same until 11p.m. We are going to compute this hourly mean for the data given by the schemes, and with the observed data. In this way, we have 3 strings (one for each scheme and one string for the real data) of 24 places.

In order to compare the schemes with the real data, we can plot the 3 hourly means in the same plot and compare which scheme is closer to the observed data. For having an idea of how far we are, we use 2 statistical errors: the Mean Bias and the Root Mean Square Error (MBE and RMSE, equations 1 and 2 respectively). The MBE is an idea of how exact is a result. For example, we could have two points with a large error, one too large and the other too short compared with the expected value. Then, the MBE of those two points will be small. Otherwise, the RMSE is an idea of how precise is a mesure, since in the example proposed before, the RMSE would be large. We will apply these statistical errors between the hourly means predicted by the schemes with the observed data.

$$MBE = \frac{\sum_{i=0}^{N} (O_i - P_i)}{N}, \tag{1}$$

$$RMSE = \sqrt{\frac{\sum_{i=0}^{N} (O_i - P_i)^2}{N}}, \tag{2}$$

Where the P_i stands for the predicted data, the O_i for the observed data and N is the number of outputs.

In that project, we have too many stations to plot all the graphics and studying it one by one. Therefore, we will plot only two stations for each air pollutant: the one with the best prediction and the one with the worst. In this graphic, we plot the 3 hourly means, as well as the PBLH predicted for each scheme. In the vertical axis, we put the concentration of the air pollutant and, in the horizontal, the hours of the day. Moreover, we draw a second axis to the right for the PBLH. If we can see the mean evolution of the pollutants and the PBLH at the same time, we can observe if the concentration fulfills the expected behavior. We compute as well the standard deviation for each hourly mean for the observed data and we also add it at the graphic.

We recall that for the pollutants CO, NO and NO_2, it is expected that their graphics must present a peak between the last hours of the stable regime of the atmosphere and in the morning residual regime; later, when the PBLH grows, the concentration of the air pollutant decreases. As the

O_3 and PM_{10}[†] are secondary air pollutants and they are created by means of sun-light, their concentrations increase during the light-time of the day. Therefore, it is expected for the O_3 and PM_{10} that they present the peak of the concentration during the convective regime of the atmosphere.

4.3 The summary table

In this table, we are going to write the MBE and the RMSE for all the stations ordered in ascending order with the value of the MBE for the BouLac. After the table, we will write the number of schemes that have a better prediction for each statistical error and we will extract conclusions. We will show one table for the weekdays and one for the weekends in order to see if there is a correlation between the predictions of the schemes and the days of the week.

In the case of the CO, the MYJ scheme is clearly the best scheme. For that reason, we will not write the RMSE, even though we will write the mean of the concentration for all day. With that average, we will be able to compare the error with the mean and see how small or large the error is.

4.4 The map

This graphic is a visual tool for placing all the stations for each air pollutant and show which scheme has worked better. Moreover, we use the markers diamond, the triangle and the circle to indicate if the station is in the urban, peri-urban or in a rural zone, respectively.

5 Results

In this section, we present the results that we have obtained from the model and the comparison with the experimental data. As we said, we will split the results by the air pollutants and we will follow the steps explained in the previous section.

5.1 Vertical Profiles

In this part of the project, we will compare and examine the vertical profile of the concentration in the city of Barcelona for all the air pollutants.

Looking at the behavior of all the pollutants (the red line of the figures 6, 7, 8, 9) and 10), the first thing that we notice is that all the pollutants show the same pattern: all of them present one pronounced peak and one valley for each day (except for the PM_{10}, that behavior does not appear so clearly for it, figure 10). However, as we expected, the peaks presented for the O_3 are not located at the same time as for the CO, NO and NO_3. The days of the week written in the horizontal axis are placed under the 00:00a.m. of the day; with that as the reference, we can compare that the concentration of one day for the CO, the NO and the NO_2 is reaching the peak passed midnight, whereas the O_3 is reaching its peak before midnight. The behavior

[†]Not all the particles that are included in the PM_{10} behave as we say here, but many of them.

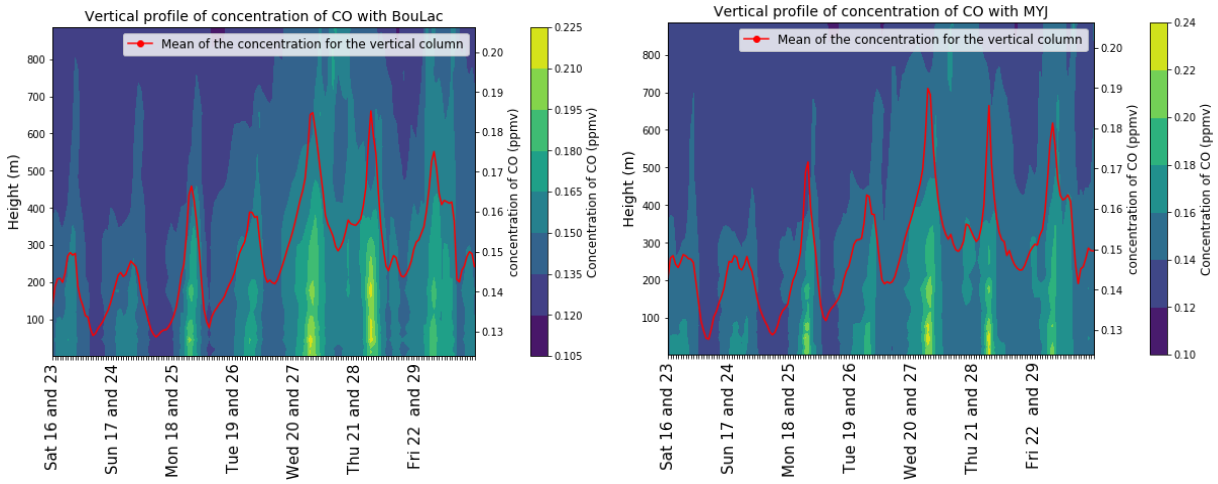

(a) Vertical profile for the CO in Barcelona computed with the BouLac PBL scheme.

(b) Vertical profile for the CO in Barcelona computed with the MYJ PBL scheme.

Figure 6: Vertical profiles for CO in the city of Barcelona.

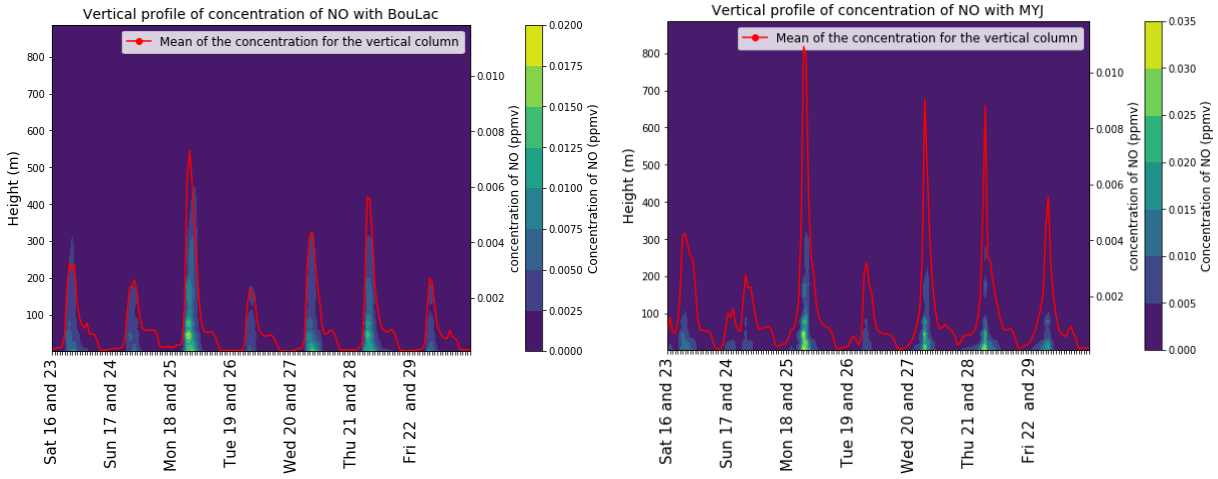

(a) Vertical profile for the NO of the city of Barcelona computed by BouLac PBL scheme.

(b) Vertical profile for the NO of the city of Barcelona computed by MYJ PBL scheme.

Figure 7: Vertical profiles for NO in the city of Barcelona.

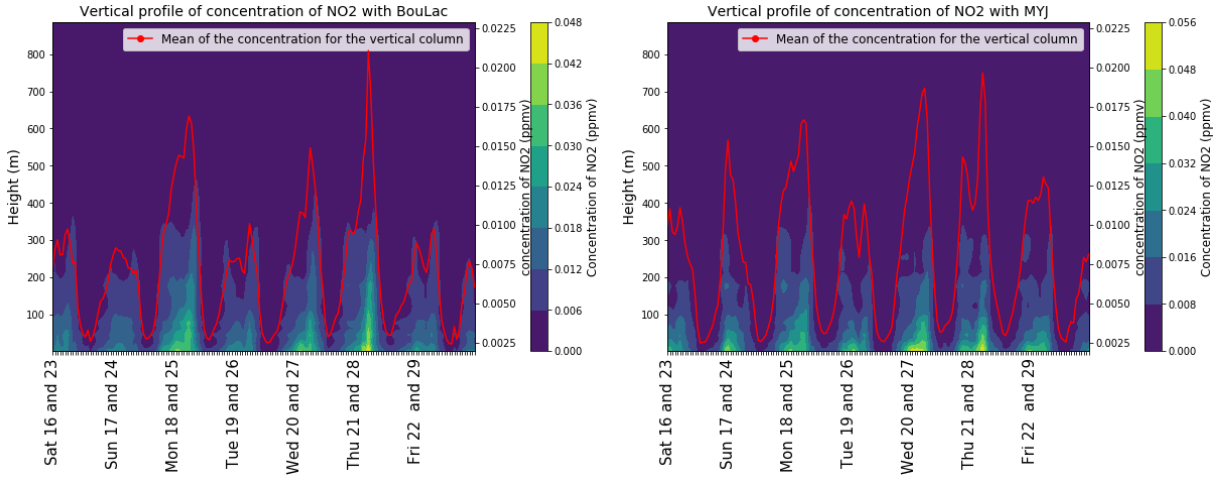

(a) Vertical profile for the NO_2 in the city of Barcelona computed by BouLac PBL scheme.

(b) Vertical profile for the NO_2 in the city of Barcelona computed by MYJ PBL scheme.

Figure 8: Vertical profiles for NO_2 in the city of Barcelona.

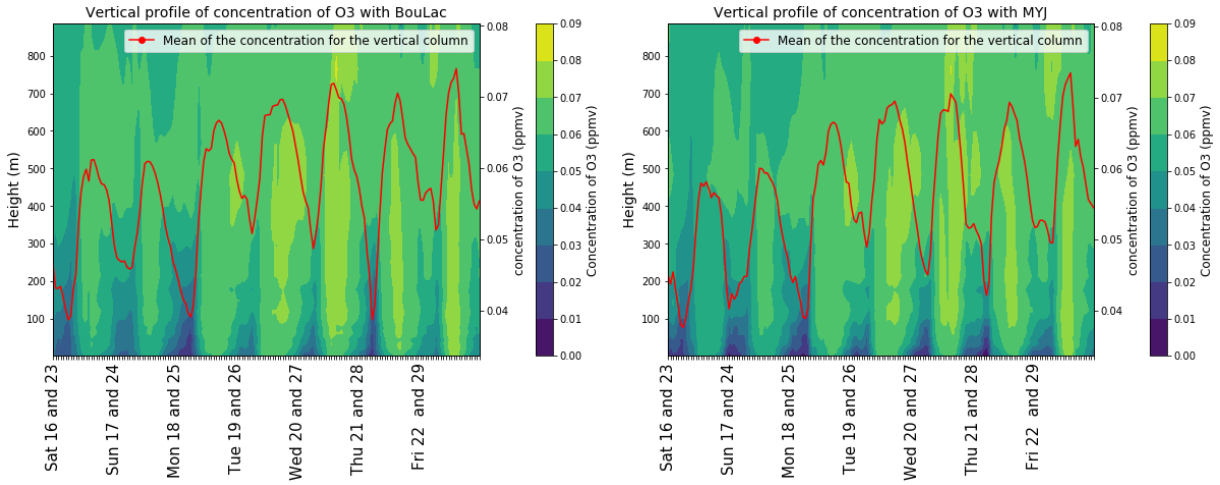

(a) Vertical profile for the O_3 in the city of Barcelona computed by BouLac PBL scheme.

(b) Vertical profile for the O_3 in the city of Barcelona computed by MYJ PBL scheme.

Figure 9: Vertical profiles for the O_3 in the city of Barcelona.

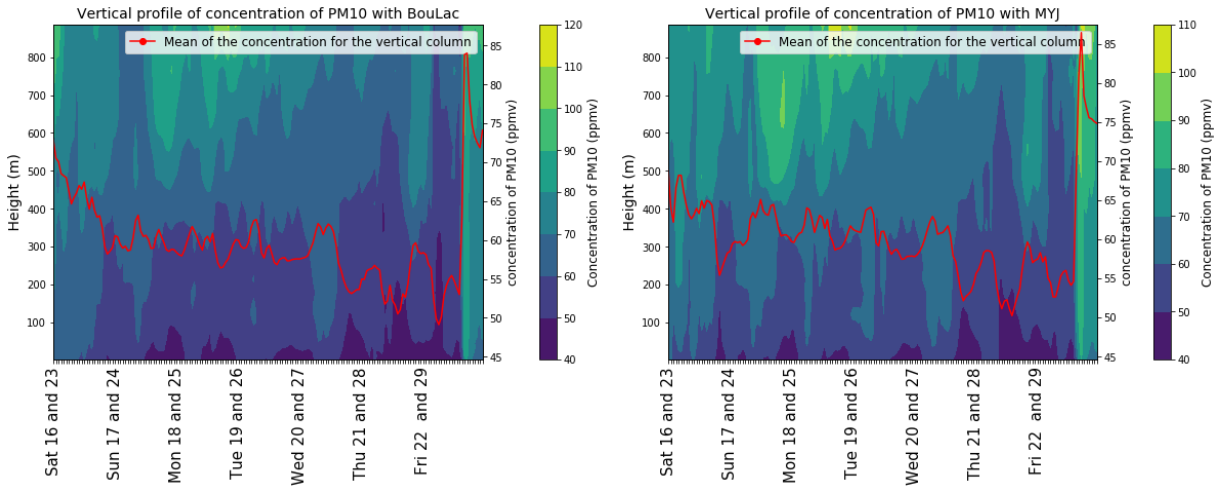

(a) Vertical profile for the $PM10_3$ in the city of Barcelona computed by BouLac PBL scheme.

(b) Vertical profile for the PM_{10} in the city of Barcelona computed by MYJ PBL scheme.

Figure 10: Vertical profiles for the PM_{10} in the city of Barcelona.

of the PM_{10} is not so well defined, although we see that the PM_{10} concentration is decreasing during the week and reaches one pronounced peak on Saturday nights.

If we focus on the CO graphics, figure 6, we see that there are no large significant differences between schemes. The things that we extract is that the CO concentration is lower during the weekend and that the MYJ scheme, figure 6b, present higher peaks, as we expect for the discussion about the PBLH predicted for both schemes.

Comparing the figures 7a and 7b, for the NO, we notice that both schemes predict the same pattern. Despite of that, the MYJ scheme presents a higher concentration at peak hours. Besides, for the NO and NO_2, the days of the weekend are not the days with the smaller contamination, as opposite to CO and O_3. Moreover, both schemes predict an almost null concentration at nights for the NO. As we said, the nitrogen oxides are strongly related to the emissions due to their short light time, for that reason, there is an almost zero concentration at night.

For the NO_2, figure 8, even though both schemes show the same pattern again, we observe significant differences between both schemes: the MYJ present pronounced peaks on Sundays and Fridays that they are not observed in the BouLac figure8a. Moreover, this time is the BouLac scheme who predicts a higher concentration of the air pollutant, as opposite to the expected. It may be due to the differences among the schemes when they treat the chemical reactions with the ozone.

When we look at the ozone and at the PM_{10} vertical profiles (figures 9 and 10, respectively), we observe that both schemes predict similar results. Both schemes place the peaks and the valleys

at the same time for both pollutants and approximately of the same height. For the case of O_3, the BouLac scheme presents a deeper valley at Thursday night (figure 9a).

5.2 The comparison with real data

5.2.1 CO

One time observed the similarities and the differences between the schemes, we use the real data so as to know which scheme gives us the best prediction. In that part, we use the hourly mean for the weekdays and for the weekends that we explained in section 4.2. Moreover, we have computed the MBE between the results of the BouLac and MYJ with the observed data. We show them in table 2. As we said, for the CO, we have computed the average of the concentration for the entire day using the observed data. With that result, we observe that there are some errors (MBE) with the same order of magnitude as the results. In the table, we have ordered the stations in ascending order with the value of the MBE for the BouLac.

City (station)	**MBE BouLac** (μg/m^3)	**MBE MYJ** (μg/m^3)	**Daily mean of the real data** (μg/m^3)	**Scheme**
Barcelona (Parc Vall Hebron)	30.004	22.436	200.000	MYJ
Viladecans - Atrium	44.713	39.325	206.250	MYJ
Gava	47.277	42.651	208.333	MYJ
Prat de Llobregat (Sagnier)	74.590	71.412	235.417	MYJ
Montcada i Reixac	80.059	71.414	256.522	MYJ
Barcelona (Palau Reial)	81.317	79.629	252.083	MYJ
Barcelona (Eixample)	225.634	220.871	401.042	MYJ
Barcelona (Gracia - Sant Gervasi)	503.518	499.657	678.261	MYJ

Table 2: Table with the MBE and the RMSE for the comparison between BouLac and MYJ for the CO on the weekdays .

Looking at the table 2, we notice that all the signs are positive for the MBE despite the scheme. This means that the predicted data is mainly below of the observed (we can see two examples of it in figures 11a and 11b). Another thing that we can note down is that if we compare the daily mean with the error, we can see that the order of the error for the last two stations is the same that the order of the daily mean. The error of these stations might be due to that these stations are located in crowded places, where the traffic jam is a common situation. Finally, we conclude that the MYJ scheme is who presents the smallest errors for all the stations when we model the CO.

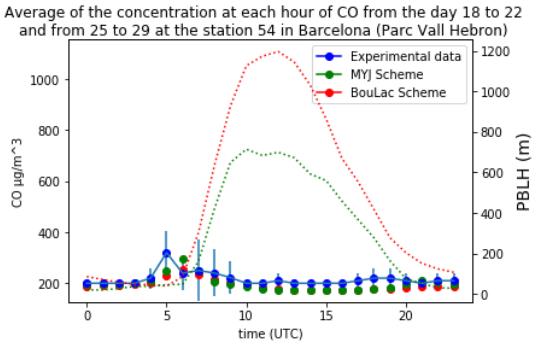

(a) Hourly mean using the model outputs of the weekdays for Vall d'Hebron station.

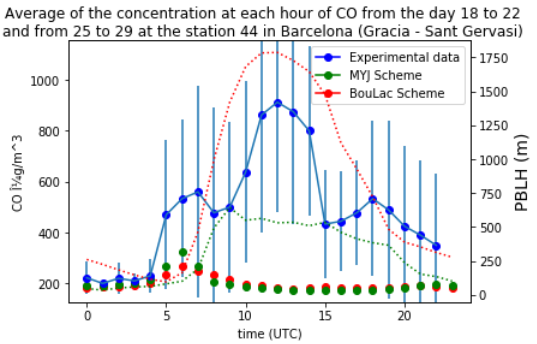

(b) Hourly mean using the model outputs of the weekdays for the Sant Gervasi station.

Figure 11: The best and the worst result for the CO.

Comparing the best and the worst station for the CO (figure 11), we can see that the schemes predict a similar behavior in both stations. However, the observed concentration of CO in Gracia station is between 3 and 5 times greater than the predicted. This station is placed in a crowded place where lots of cars travel around. We can conclude that the model have not represented the amount of emissions for these places. On the other hand, the concentration for the Vall d'Hebron follows the expected behavior: when the PBLH grows, the concentration must decreass. We can also see that the MYJ scheme presents a more pronounced peak than the BouLac data in both stations. In addition, the figures show that the PBLH simulated for the BouLac (dotted line in red) is higher than the predicted with the MYJ (green dotted line).

We follow the study with the maps where we locate the stations of Barcelona and the metropolitan area for the CO (one map using the MBE and the other using the RMSE). In the maps, we paint the points in blue for the stations in which the MYJ scheme is better, and with red for the BouLac (figure 12). We have a summary table (table 4) where we can observe possible correlations extracted from the map.

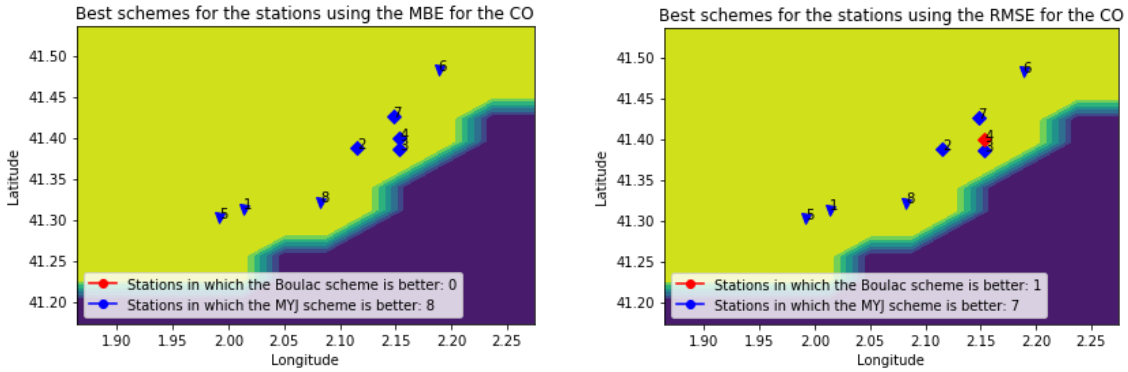

(a) Map of the metropolitan area showing the best scheme for each station using the MBE.

(b) Map of the metropolitan area showing the best scheme for each station using the RMSE.

Figure 12: Map placing the stations with the best scheme for each one. We can see the cities in the table 3. The $\diamond$ is for urban zones, $\triangledown$ for the periurban and the *o* for the rural.

Num	**City (station)**
1	Viladecans - Atrium
2	Barcelona (Palau Reial)
3	Barcelona (Eixample)
4	Barcelona (Gracia - Sant Gervasi)
5	Gava
6	Montcada i Reixac
7	Barcelona (Parc Vall Hebron)
8	Prat de Llobregat (Sagnier)

Table 3: Cities of the map of the figure 12

	Zone		**Urban region**		
	Metropolitan Area	**Barcelona**	**Urban**	**Periurban**	**Rural**
MBE					
Proportion of stations (B/M)	0 / 4	0 / 4	0 / 4	0 / 4	0 / 0
RMSE					
Proportion of stations (B/M)	0 / 4	1 / 3	1 / 3	0 / 4	0 / 0

Table 4: Summary table for the map of the figure 12.

For the CO there is no doubt about that the MYJ scheme is the scheme that better represents the reality. In the map of the figure 12, we can see that the stations 3 and 4 (Eixample and Gracia) are located in the middle of the city, and both are the stations which present the biggest

error.

Finally, we add the results for the weekend for the CO ploting another table as the table 2. Despite of the fact that the best scheme is still the MYJ, the order of the stations have changed. Therefore, it is true that we have different predictions depending on studying the weekends or the weekdays.

City (station)	**MBE BouLac** ($\mu g/m^3$)	**MBE MYJ** ($\mu g/m^3$)	**Daily mean concentration for the real data** ($\mu g/m^3$)	**Scheme**
Barcelona (Parc Vall Hebron)	22.811	17.040	215.926	MYJ
Montcada i Reixac	33.939	26.434	231.932	MYJ
Barcelona (Palau Reial)	34.001	34.967	228.935	BouLac
Viladecans - Atrium	61.806	57.467	244.544	MYJ
Gava	67.011	63.165	247.384	MYJ
Prat de Llobregat (Sagnier)	85.659	82.953	267.963	MYJ
Barcelona (Gracia - Sant Gervasi)	290.283	289.714	489.287	MYJ
Barcelona (Eixample)	411.397	410.831	608.194	MYJ

Table 5: Table with the MBE and the RMSE for the comparison between BouLac and MYJ for the CO at the weekend..

The conclusion for the CO is that the best scheme to represent the reality is the MYJ.

5.2.2 NO

Following with the study for the NO, we start the comparation between both schemes with the table 6. In this, we show the MBE and the RMSE for the results of both schemes for each station. We observe again how the Gracia and Eixample stations are the stations with the worst prediction (the ones who are in the middle of Barcelona). The Vall Hebron stations, which is near to the Natural Parc of Collserola, is again between the stations which obtain better predictions. In the discussion of the map of the stations and their best scheme (figure 14), we will go deep with the correlations between best scheme with the urban region and with the location of the station.

The discussion for the NO continues with the plots showing the hourly mean concentration for the best station (Hospitalet de Llobregat) and the worst (Eixample). In figure 13a, the Hospitalet de Llobregat one, we observe how the hourly concentration follow the expected behavior: it grows when the PBLH is shorter until the concentration reaches its peak, and then it starts to decreasse. Both peaks predicted by the model are higher than the observed, although the MYJ peak is much higher. On the other hand, in figure 13b, the one for the Eixample, we find the same problem that with the concentration of CO for Gracia: in the stations of Gracia and Eixample, the real emissions are so high that the HERMES (the antrhopogenic inventory emission) does not predict the amount of concentrations that these stations have. Nevertheless,

City (station)	**MBE BouLac/MBE MYJ (scheme)** ($\mu g/m^3$)	**RMSE BouLac/ RMSE MYJ (scheme)** ($\mu g/m^3$)
Hospitalet de Llobregat	0.134 / 0.433 (BouLac)	1.255 / 2.061 (BouLac)
Barcelona (Parc Vall Hebron)	0.186 / 0.676 (BouLac)	1.019 / 1.290 (BouLac)
Sant Cugat del Valles	0.206 / 0.585 (BouLac)	0.831 / 1.141 (BouLac)
Sant Feliu de Ll. (CEIP Marti i Pol)	0.214 / 0.353 (BouLac)	0.837 / 0.884 (BouLac)
Barcelona (Ciutadella)	0.511 / 4.880 (BouLac)	3.411 / 9.099 (BouLac)
Barcelona (Poblenou)	0.778 / 0.585 (MYJ)	2.034 / 3.339 (BouLac)
Gava	0.841 / 0.731 (MYJ)	1.064 / 1.101 (BouLac)
Barcelona (Palau Reial)	1.043 / 0.744 (MYJ)	1.656 / 2.288 (BouLac)
Viladecans - Atrium	1.083 / 1.016 (MYJ)	1.206 / 1.107 (MYJ)
Palleja (Roca de Vilana)	1.170 / 1.052 (MYJ)	1.493 / 1.308 (MYJ)
Barbera del Valles	1.664 / 1.018 (MYJ)	4.507 / 4.464 (MYJ)
El Prat (Jardins de la Pau)	1.755 / 0.946 (MYJ)	3.050 / 2.670 (MYJ)
Barcelona (Sants)	1.773 / 1.473 (MYJ)	2.137 / 2.791 (BouLac)
Sta Coloma de Gramenet	2.390 / 1.900 (MYJ)	3.465 / 2.880 (MYJ)
Badalona	2.621 / 1.995 (MYJ)	2.978 / 2.407 (MYJ)
Sant Vicenc dels Horts	2.754 / 2.635 (MYJ)	4.398 / 4.165 (MYJ)
Sant Adria de Besos	2.820 / 2.331 (MYJ)	5.083 / 4.359 (MYJ)
Sant Vicenc dels Horts (Ribot)	3.093 / 2.930 (MYJ)	4.016 / 3.725 (MYJ)
Montcada i Reixac	3.159 / 1.913 (MYJ)	5.056 / 3.865 (MYJ)
Prat de Llobregat (Sagnier)	3.855 / 3.837 (MYJ)	4.600 / 4.473 (MYJ)
Barcelona (Gracia - Sant Gervasi)	5.614 / 4.405 (MYJ)	6.179 / 5.558 (MYJ)
Barcelona (Eixample)	10.376 / 7.395 (MYJ)	12.568 / 14.975 (BouLac)

Table 6: Table with the MBE and the RMSE for the comparison between BouLac and MYJ for the NO on the weekdays .

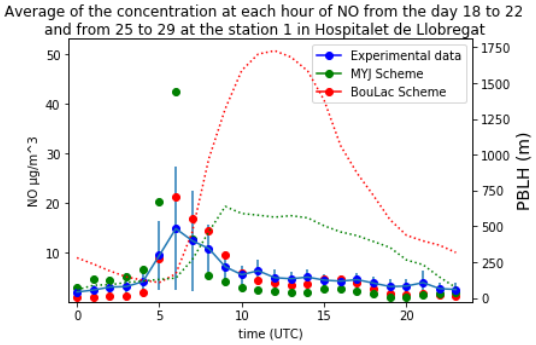

(a) Hourly mean using the model outputs of the weekdays for the Hospitalet de Llobregat station.

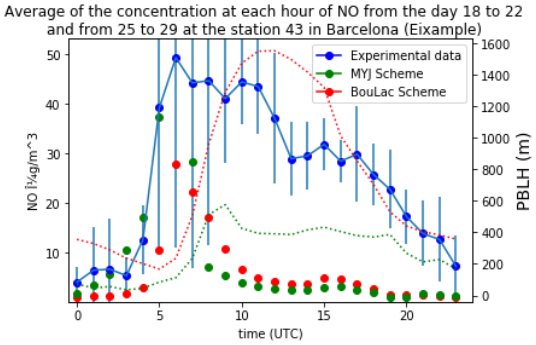

(b) Hourly mean using the model outputs of the weekdays for for the Eixample station.

Figure 13: The best and the worst predicted data for the NO.

in that case it is respected the expected behavior of the concentration (for the observed and the simulated data). This time, the model have predicted a greater amount of concentration during the peak hours than when we model the CO (for the crowded stations).

In the next step, we will locate the stations on the map and mark which scheme has been better for each station (figure 14). In the maps, we can see that the stations at the middle of Barcelona city change their color. In the table 8, we observe that the MYJ is a better scheme for modelling periurban zones and stations outside the city of Barcelona. However, for the Urban zones and for stations inside Barcelona, the conclusion is not so clear. Inside Barcelona, the RMSE predicts that the best scheme is the BouLac, whereas using the MBE the best scheme is the MYJ. For that reason, we can not extract strong conclusions in the urban zones.

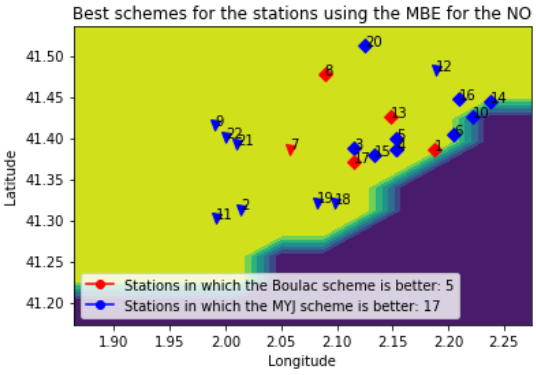

(a) Map of the metropolitan area of Barcelona showing the best scheme for each station using the MBE.

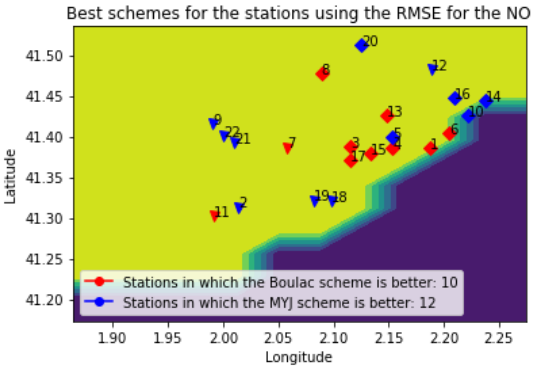

(b) Map of the metropolitan area of Barcelona showing the best scheme for each station using the RMSE.

Figure 14: Map placing the stations with the best scheme for each one for the NO. We can see the cities in the table 7. The $\diamond$ is for urban zones, $\triangledown$ for the periurban and the o for the rural.

Num	City (station)	Num	City (station)
1	Barcelona (Ciutadella)	12	Montcada i Reixac
2	Viladecans - Atrium	13	Barcelona (Parc Vall Hebron)
3	Barcelona (Palau Reial)	14	Badalona
4	Barcelona (Eixample)	15	Barcelona (Sants)
5	Barcelona (Gracia - Sant Gervasi)	16	Sta Coloma de Gramenet
6	Barcelona (Poblenou)	17	Hospitalet de Llobregat
7	Sant Feliu de Ll. (CEIP Marti i Pol)	18	El Prat (Jardins de la Pau)
8	Sant Cugat del Valles	19	Prat de Llobregat (Sagnier)
9	Palleja (Roca de Vilana)	20	Barbera del Valles
10	Sant Adria de Besos	21	Sant Vicenc dels Horts (Ribot)
11	Gava	22	Sant Vicenc dels Horts

Table 7: Table referencing the stations in the figure 14

	Zone		**Urban region**		
	Metropolitan Area	**Barcelona**	**Urban**	**Periurban**	**Rural**
MBE					
Proportion of stations (B/M)	3 / 12	2 / 5	4 / 9	1 / 8	0 / 0
RMSE					
Proportion of stations (B/M)	4 / 11	6 / 1	8 / 5	2 / 7	0 / 0

Table 8: Summary table for the map of the figure 14 for the NO.

Looking at the table 9, we can extract conclusions for the differences between the weekdays and the weekends. Outside Barcelona, using the MBE, we have 13 stations for the MYJ against 2 for the BouLac. Using the RMSE, 12 for the MYJ and 3 for BouLac. Then, we can conclude that, outside Barcelona, the best scheme is the MYJ at the weekends too. However, inside Barcelona, using the MBE we have 4 MYJ against 3 Boulac and using the RMSE we have 1 MYJ against 6 BouLac. Another flashy fact is that the errors observed at the weekend are much larger than the observed during the weekdays.

City (station)	**MBE BouLac/MBE MYJ (scheme)** ($\mu g/m^3$)	**RMSE BouLac/ RMSE MYJ (scheme)** ($\mu g/m^3$)
Sant Feliu de Ll. (CEIP Marti i Pol)	0.097 / 0.447 (BouLac)	2.207 / 3.956 (BouLac)
Hospitalet de Llobregat	0.259 / 0.331 (BouLac)	2.213 / 6.496 (BouLac)
Barcelona (Palau Reial)	0.730 / 1.320 (BouLac)	2.430 / 6.338 (BouLac)
Sant Cugat del Valles	1.314 / 0.460 (MYJ)	3.012 / 3.381 (BouLac)
Barcelona (Sants)	1.395 / 1.985 (BouLac)	2.898 / 6.933 (BouLac)
Barcelona (Parc Vall Hebron)	1.422 / 0.358 (MYJ)	3.906 / 6.079 (BouLac)
Barcelona (Ciutadella)	1.665 / 3.015 (BouLac)	3.855 / 11.955 (BouLac)
Gava	1.768 / 1.557 (MYJ)	2.935 / 2.464 (MYJ)
Viladecans - Atrium	2.637 / 2.378 (MYJ)	3.266 / 2.724 (MYJ)
Sta Coloma de Gramenet	3.130 / 1.622 (MYJ)	4.164 / 3.957 (MYJ)
Palleja (Roca de Vilana)	4.337 / 3.863 (MYJ)	9.432 / 7.783 (MYJ)
Sant Adria de Besos	5.284 / 3.777 (MYJ)	10.677 / 8.509 (MYJ)
Badalona	5.430 / 4.154 (MYJ)	6.834 / 4.899 (MYJ)
Barcelona (Poblenou)	5.739 / 3.239 (MYJ)	9.250 / 6.488 (MYJ)
Sant Vicenc dels Horts	6.528 / 6.054 (MYJ)	15.149 / 13.628 (MYJ)
Barbera del Valles	6.672 / 4.646 (MYJ)	14.063 / 11.911 (MYJ)
El Prat (Jardins de la Pau)	7.379 / 4.989 (MYJ)	16.171 / 11.975 (MYJ)
Montcada i Reixac	7.972 / 5.699 (MYJ)	16.045 / 12.212 (MYJ)
Prat de Llobregat (Sagnier)	9.669 / 8.926 (MYJ)	16.038 / 14.175 (MYJ)
Sant Vicenc dels Horts (Ribot)	9.981 / 9.460 (MYJ)	20.565 / 19.116 (MYJ)
Barcelona (Gracia - Sant Gervasi)	15.122 / 13.367 (MYJ)	15.905 / 16.090 (BouLac)
Barcelona (Eixample)	20.159 / 16.956 (MYJ)	22.772 / 23.415 (BouLac)

Table 9: Table with the MBE and the RMSE for the comparison between BouLac and MYJ for the NO at the weekend.

5.2.3 NO_2

Following the guideline again for the results, we start the comparison between the schemes for the NO_2 with the table 10. In the figure 16, we will discuss and locate all the stations of the table and we will look for correlations between the best scheme with the urban zone and with the location. The best station now is the station of El Prat (Jardins de la Pau, with an MBE for the MYJ scheme of 0,156 $\mu g/m^3$, whereas the worst is Gracia, with a RMSE of 32.143$\mu g/m^3$ for the predictions BouLac. The following step is comparing these stations. We can see them in figure 15.

In the left image, figure 15a, we observe how for, from 5 on, both schemes predict almost all the points within the error lines for the observed data. The MYJ scheme starts being too high, whereas the BouLac fails on the concentration of the peak hours. We see how all the data follows the expected behavior for the NO_2. In contrast, the observed data of the figure 15b, does not fulfill so clearly the expected behavior. We can note down that the predicted data always fulfill the expected behavior. The problem that in the crowded stations, the emissions affect to the expected behavior for the air pollutants. In that cases, both model compute predictions with large errors.

City (station)	**MBE BouLac/MBE MYJ (scheme) ($\mu g/m^3$)**	**RMSE BouLac/ RMSE MYJ (scheme) ($\mu g/m^3$)**
Barcelona (Parc Vall Hebron)	0.186 / 7.854 (BouLac)	6.385 / 14.559 (BouLac)
Sant Cugat del Valles	2.835 / 9.114 (BouLac)	5.726 / 16.520 (BouLac)
Barcelona (Ciutadella)	2.912 / 12.393 (BouLac)	10.024 / 23.325 (BouLac)
Barcelona (Eixample)	3.444 / 0.023 (MYJ)	15.147 / 28.157 (BouLac)
Montcada i Reixac	3.750 / 3.723 (MYJ)	7.067 / 10.956 (BouLac)
Barcelona (Poblenou)	4.182 / 4.414 (BouLac)	7.277 / 14.545 (BouLac)
El Prat (Jardins de la Pau)	4.211 / 0.411 (MYJ)	6.582 / 9.244 (BouLac)
Gava	4.284 / 7.384 (BouLac)	8.379 / 12.762 (BouLac)
Viladecans - Atrium	4.658 / 8.474 (BouLac)	6.715 / 13.053 (BouLac)
Palleja (Roca de Vilana)	4.751 / 0.882 (MYJ)	6.643 / 9.046 (BouLac)
Barcelona (Gracia - Sant Gervasi)	5.206 / 0.658 (MYJ)	8.662 / 20.112 (BouLac)
Hospitalet de Llobregat	6.134 / 6.625 (BouLac)	8.207 / 17.597 (BouLac)
Badalona	6.205 / 0.037 (MYJ)	8.782 / 5.316 (MYJ)
Sant Vicenc dels Horts	7.251 / 3.382 (MYJ)	10.490 / 9.292 (MYJ)
Sta Coloma de Gramenet	7.416 / 1.023 (MYJ)	11.161 / 7.624 (MYJ)
Sant Feliu de Ll. (CEIP Marti i Pol)	7.951 / 11.972 (BouLac)	10.056 / 16.242 (BouLac)
Barbera del Valles	8.598 / 2.523 (MYJ)	13.869 / 13.357 (MYJ)
Prat de Llobregat (Sagnier)	8.833 / 6.467 (MYJ)	12.003 / 7.510 (MYJ)
Barcelona (Palau Reial)	8.863 / 9.354 (BouLac)	9.931 / 19.603 (BouLac)
Sant Vicenc dels Horts (Ribot)	8.922 / 4.340 (MYJ)	12.567 / 12.284 (MYJ)
Barcelona (Sants)	10.103 / 10.594 (BouLac)	11.875 / 20.731 (BouLac)
Sant Adria de Besos	11.010 / 4.617 (MYJ)	15.368 / 7.531 (MYJ)

Table 10: Table with the MBE and the RMSE for the comparison between BouLac and MYJ for the NO_2 on the weekdays .

We follow with the discussion of the figure 16, and the possible correlations showed in the table 12. The possible strong correlations that we can extract is that the BouLac is the best scheme for modeling stations within Barcelona, as both statistical errors agree it. The other possibles correlations are not fulfilled for the NO_2.

The resume of the table is that we have using the MBE 5 stations for BouLac against 10 for the MYJ in the metropolitan area whereas we have five stations for BouLac against two for the MYJ inside Barcelona; using the RMSE we have 8 stations for BouLac outside Barcelona against 7 for the MYJ, while in Barcelona city we have no stations for MYJ against 8 for BouLac. The conclusion is that is not clear outside Barcelona which is the best scheme, but in Barcelona the best scheme has been the BouLac.

Finally, we are going to show the table 11 for the weekend, for the NO_2, in order to see if there is differences between the weekdays. If we count the stations, that time we have in the metropolitan area 4 for the BouLac against 11 for the MYJ, using the MBE, and 6 for BouLac against 9 for the MYJ, using the RMSE. At the weekend, it seems that there is a more clear

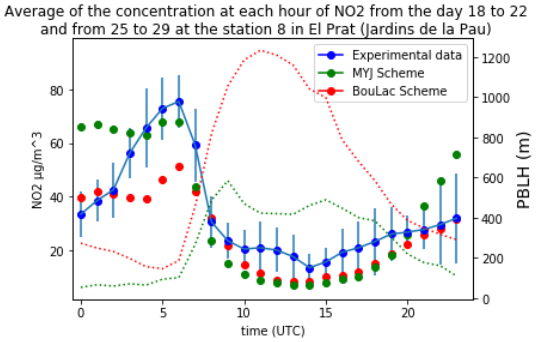

(a) Hourly mean using the model outputs of the weekdays for El Prat (Jardins de la Pau) station.

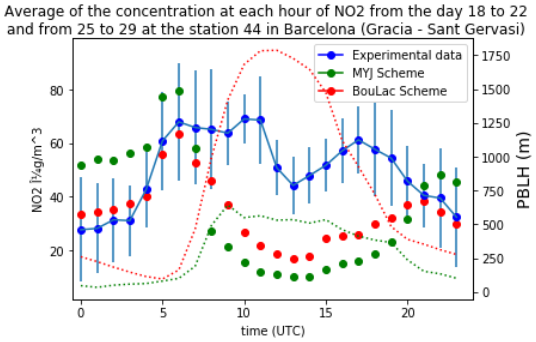

(b) Hourly mean using the model outputs of the weekdays for the Gracia station.

Figure 15: The best and the worst predicted data for the NO_2.

correlation between the MYJ and the cities outside Barcelona. However, inside Barcelona, we have, using the MBE, 3 stations for the BouLac against 4 for the MYJ, and, using the RMSE, we have 7 for the BouLac against 0 for the MYJ. The correlation between BouLac and the best results within Barcelona is not so clear for the weekends as for the weekdays.

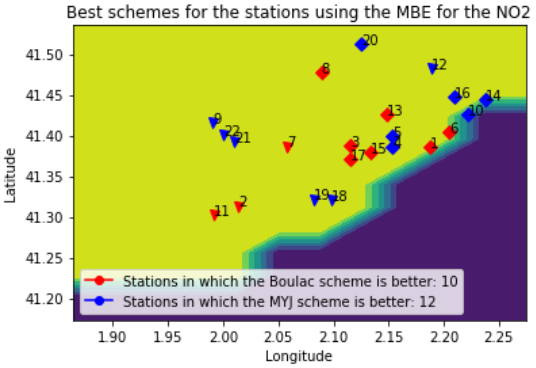

(a) Map of the metropolitan area of Barcelona showing the best scheme for each station using the MBE.

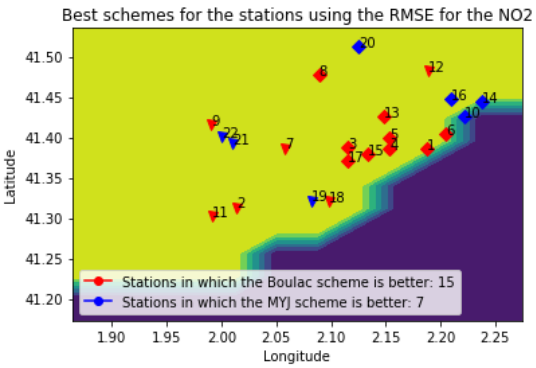

(b) Map of the metropolitan area of Barcelona showing the best scheme for each station using the RMSE.

Figure 16: Map placing the stations with the best scheme for each one. We can see the cities in the table 7, we use the same table as for the NO because they have the same stations. The $\diamond$ is for urban zones, $\triangledown$ for the periurban and the o for the rural.

5.2.4 O_3

We focus our attention now to the ozone. Again, we show the table with the values of the MB and the RMS errors, besides the best scheme for each station (table 13). We observe that the MYJ predomines over BouLac with both statistcal errors. The best station predicted by the MYJ is Barcelona (Ciutadella), with a MBE of 1.540 $\mu g/m^3$; whereas the worst is the Prat

City (station)	**MBE BouLac/MBE MYJ (scheme) ($\mu g/^3$)**	**RMSE BouLac/ RMSE MYJ (scheme) ($\mu g/m^3$)**
Barcelona (Ciutadella)	0.541 / 6.295 (BouLac)	13.914 / 22.196 (BouLac)
Viladecans - Atrium	1.171 / 5.842 (BouLac)	5.122 / 12.049 (BouLac)
Gava	1.725 / 6.232 (BouLac)	7.323 / 12.681 (BouLac)
Sant Feliu de Ll. (CEIP Marti i Pol)	4.432 / 9.646 (BouLac)	8.131 / 15.897 (BouLac)
Sant Cugat del Valles	5.071 / 0.652 (MYJ)	7.438 / 9.610 (BouLac)
Barcelona (Parc Vall Hebron)	6.651 / 0.261 (MYJ)	10.053 / 11.967 (BouLac)
Barcelona (Palau Reial)	7.126 / 7.515 (BouLac)	9.748 / 21.758 (BouLac)
Hospitalet de Llobregat	7.212 / 7.601 (BouLac)	9.821 / 21.416 (BouLac)
El Prat (Jardins de la Pau)	7.935 / 0.156 (MYJ)	11.739 / 14.090 (BouLac)
Palleja (Roca de Vilana)	8.631 / 4.358 (MYJ)	11.809 / 11.498 (MYJ)
Sant Vicenc dels Horts	9.678 / 5.405 (MYJ)	13.336 / 11.497 (MYJ)
Barcelona (Eixample)	10.794 / 9.050 (MYJ)	25.185 / 35.406 (BouLac)
Barcelona (Sants)	10.887 / 11.276 (BouLac)	13.076 / 23.185 (BouLac)
Sta Coloma de Gramenet	11.492 / 6.464 (MYJ)	12.420 / 11.269 (MYJ)
Montcada i Reixac	11.879 / 6.191 (MYJ)	12.552 / 11.150 (MYJ)
Barcelona (Poblenou)	13.084 / 8.976 (MYJ)	15.419 / 17.322 (BouLac)
Sant Vicenc dels Horts (Ribot)	13.141 / 8.337 (MYJ)	16.902 / 16.144 (MYJ)
Prat de Llobregat (Sagnier)	14.575 / 8.496 (MYJ)	15.865 / 10.521 (MYJ)
Sant Adria de Besos	14.872 / 9.845 (MYJ)	16.977 / 12.667 (MYJ)
Badalona	15.178 / 9.281 (MYJ)	16.197 / 12.121 (MYJ)
Barbera del Valles	15.264 / 9.985 (MYJ)	16.894 / 13.647 (MYJ)
Barcelona (Gracia - Sant Gervasi)	16.265 / 14.719 (MYJ)	22.788 / 32.143 (BouLac)

Table 11: Table with the MBE and the RMSE for the comparison between BouLac and MYJ for the NO_2 at the weekend.

	Zone		**Urban region**		
	Metropolitan Area	**Barcelona**	**Urban**	**Periurban**	**Rural**
MBE					
Proportion of stations (B/M)	5 / 10	5 / 2	7 / 6	3 / 6	0 / 0
RMSE					
Proportion of stations (B/M)	8 / 7	7 / 0	9 / 4	6 / 3	0 / 0

Table 12: Summary table for the map of the figure 16

City (station)	**MBE BouLac/MBE MYJ (scheme) (μg/m^3)**	**RMSE BouLac/ RMSE MYJ (scheme) (μg/m^3)**
Barcelona (Palau Reial)	2.591 / 4.753 (BouLac)	8.087 / 15.394 (BouLac)
Barcelona (Parc Vall Hebron)	4.878 / 7.242 (BouLac)	12.915 / 12.786 (MYJ)
Barcelona (Ciutadella)	10.400 / 1.540 (MYJ)	17.359 / 16.144 (MYJ)
Barcelona (Eixample)	14.097 / 9.054 (MYJ)	17.819 / 25.341 (BouLac)
Sant Cugat del Valles	14.568 / 4.674 (MYJ)	20.235 / 8.062 (MYJ)
Badalona	16.483 / 6.345 (MYJ)	23.486 / 14.502 (MYJ)
Barcelona (Gracia - Sant Gervasi)	16.724 / 10.081 (MYJ)	20.100 / 21.537 (BouLac)
Viladecans - Atrium	19.455 / 11.825 (MYJ)	22.236 / 14.543 (MYJ)
Sant Adria de Besos	24.198 / 14.326 (MYJ)	30.846 / 18.924 (MYJ)
Montcada i Reixac	24.893 / 13.142 (MYJ)	31.212 / 16.131 (MYJ)
Sant Vicenc dels Horts (Ribot)	26.464 / 17.396 (MYJ)	29.392 / 20.712 (MYJ)
Gava	26.794 / 19.839 (MYJ)	31.682 / 23.002 (MYJ)
Prat de Llobregat (Sagnier)	33.712 / 29.016 (MYJ)	37.053 / 31.092 (MYJ)

Table 13: Table with the MBE and the RMSE for the comparison between BouLac and MYJ for the O_3 on the weekdays .

del LLobregat (Sagnier), with a MBE of 33,712 μg/m^3 for the MYJ. In the table 16, we have written the errors with the data of the weekends. Again, the MYJ scheme is who present more stations with a better prediction. Therefore, the best scheme for simulating the ozone is the MYJ scheme. A strong difference between the weekend and the weekdays is that the stations present larger errors for the weekend. Then, we can trust with more security in the MYJ during the weekdays.

Even though we have already decided the best scheme for the ozone, we will look for correlations between the characteristics of the stations that have better results with the BouLac scheme. We study that correlation employing the location of the stations in the map of Barcelona and separating them by their urban region (as with the previous pollutants).

Before studying the possible correlations between best schemes for the stations and their characteristics, we will observe the predicted daily behavior of the ozone (figure 17), using the stations with the best and the worst results. In both pictures, we can see the expected behavior for the ozone: instead of presenting a peak during the last hours of the night (as the nitrogen oxides and the CO), the concentration of ozone starts to grow by this time. Not only fulfills that behavior the predicted data, but also the observed. If we look at the figure 17a, we observe that, until the 9a.m., the predicted data is inside the error bars of the observed data. However, from 9a.m. on, the predicted data becomes larger than the expected. In the Sagnier station, the predicted data is always above the observed. We can see that both PBL schemes give similar results, except for the first hours of the day. In these hours, the MYJ is the best scheme.

Now we will study the correlations between the best scheme for a station and its characteristics. In figure 18, we can see that the stations that gives better results with the BouLac are inside

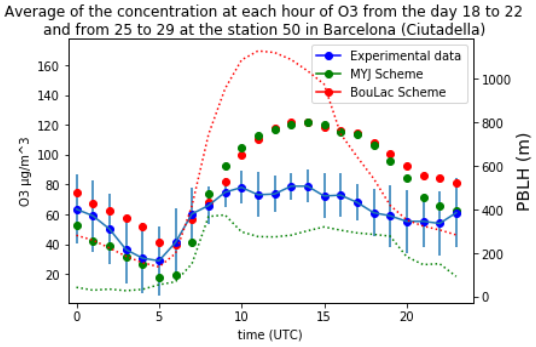

(a) Hourly mean using the model outputs of the weekdays for Barcelona (Ciudadella) station.

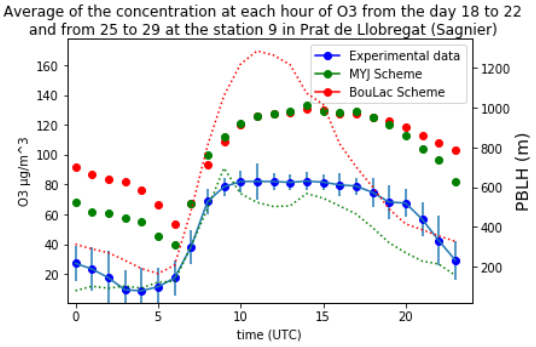

(b) Hourly mean using the model outputs of the weekdays for the Prat de Llobregat (Sagnier) station.

Figure 17: The best and the worst predicted data for the O_3.

Barcelona, but both errors do not agree in which is the best scheme for the stations of Barcelona. Therefore, we can not confirm that fact. Otherwise, we see that there are stations in urban regions, outside Barcelona, that are better predicted with the MYJ shceme. Therefore, we can go further and say that MYJ is the best scheme not only for the periurban regions, but also for the urban outside Barcelona.

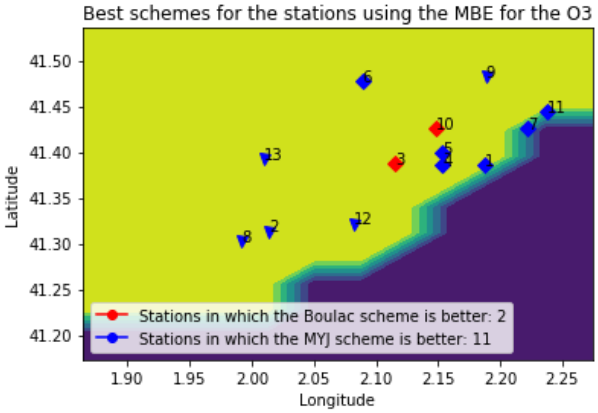

(a) Map of the metropolitan area of Barcelona showing the best scheme for each station using the MBE.

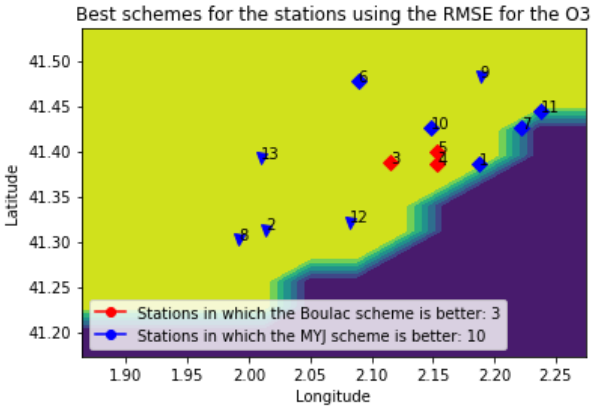

(b) Map of the metropolitan area of Barcelona showing the best scheme for each station using the RMSE.

Figure 18: Map placing the stations with the best scheme for each one for the ozone prediction. We can see the cities in the table 14. The $\diamond$ is for urban zones, $\triangledown$ for the periurban and the o for the rural.

City (station)	**MBE BouLac/MBE MYJ (scheme) (μg/m^3)**	**RMSE BouLac/ RMSE MYJ (scheme) (μg/m^3)**
Barcelona (Palau Reial)	12.792 / 11.754 (MYJ)	16.364 / 23.613 (BouLac)
Barcelona (Parc Vall Hebron)	25.450 / 16.132 (MYJ)	28.265 / 22.282 (MYJ)
Barcelona (Ciutadella)	26.041 / 16.564 (MYJ)	30.834 / 29.250 (MYJ)
Barcelona (Eixample)	32.125 / 29.253 (MYJ)	36.599 / 42.789 (BouLac)
Sant Cugat del Valles	33.095 / 27.028 (MYJ)	36.840 / 29.123 (MYJ)
Barcelona (Gracia - Sant Gervasi)	33.842 / 31.244 (MYJ)	36.582 / 42.628 (BouLac)
Badalona	37.683 / 28.234 (MYJ)	39.088 / 30.890 (MYJ)
Viladecans - Atrium	38.927 / 30.917 (MYJ)	39.870 / 32.410 (MYJ)
Sant Vicenc dels Horts (Ribot)	40.127 / 32.190 (MYJ)	41.053 / 33.820 (MYJ)
Sant Adria de Besos	41.977 / 34.205 (MYJ)	44.108 / 36.864 (MYJ)
Gava	43.415 / 34.564 (MYJ)	46.276 / 35.627 (MYJ)
Montcada i Reixac	45.018 / 36.569 (MYJ)	47.426 / 38.955 (MYJ)
Prat de Llobregat (Sagnier)	51.277 / 43.480 (MYJ)	52.935 / 44.216 (MYJ)

Table 16: Table with the MBE and the RMSE for the comparison between BouLac and MYJ for the O_3 at the weekend.

Num	**City (station)**	**Num**	**City (station)**
1	Barcelona (Ciutadella)	8	Gava
2	Viladecans - Atrium	9	Montcada i Reixac
3	Barcelona (Palau Reial)	10	Barcelona (Parc Vall Hebron)
4	Barcelona (Eixample)	11	Badalona
5	Barcelona (Gracia - Sant Gervasi)	12	Prat de Llobregat (Sagnier)
6	Sant Cugat del Valles	13	Sant Vicenc dels Horts (Ribot)
7	Sant Adria de Besos		

Table 14: Table referencing the stations in the figure 14

	Zone		**Urban region**		
	Metropolitan Area	**Barcelona**	**Urban**	**Periurban**	**Rural**
MBE					
Proportion of stations (B/M)	0 / 8	2 / 3	2 / 6	0 / 5	0 / 0
RMSE					
Proportion of stations (B/M)	0 / 8	3 / 2	3 / 5	0 / 5	0 / 0

Table 15: Summary table for the map of the figure 18

City (station)	**MBE BouLac/MBE MYJ (scheme) (μg/m^3)**	**RMSE BouLac/ RMSE MYJ (scheme) (μg/m^3)**
Sant Just Desvern (CEIP Montseny)	24.291 / 22.696 (MYJ)	26.936 / 25.822 (MYJ)
Barcelona (Poblenou)	25.581 / 24.949 (MYJ)	27.175 / 25.941 (MYJ)
Sant Vicenc dels Horts (Ribot)	27.581 / 25.995 (MYJ)	29.284 / 28.513 (MYJ)
Sant Adria de Besos	30.799 / 29.187 (MYJ)	30.997 / 29.352 (MYJ)
Barcelona (Eixample)	32.579 / 32.039 (MYJ)	33.504 / 32.664 (MYJ)
Barcelona (Gracia - Sant Gervasi)	36.105 / 35.977 (MYJ)	36.566 / 36.351 (MYJ)
Hospitalet de Llobregat	36.202 / 35.416 (MYJ)	36.493 / 35.672 (MYJ)
Montcada i Reixac	36.294 / 35.027 (MYJ)	36.945 / 35.826 (MYJ)
Barcelona (Palau Reial)	37.577 / 36.791 (MYJ)	37.817 / 37.012 (MYJ)
Montcada i Reixac (Can Sant Joan)	40.256 / 38.656 (MYJ)	40.481 / 38.988 (MYJ)
Barcelona (Parc Vall Hebron)	41.008 / 39.851 (MYJ)	41.212 / 40.107 (MYJ)

Table 17: Table with the MBE and the RMSE for the comparison between BouLac and MYJ for the PM_{10} on the weekdays .

5.2.5 PM_{10}

As all the other air pollutants, we start the comparison with the table 17. In the same, we show the errors for the predictions of both schemes. For PM_{10}, all the stations present the best prediction with the MYJ scheme. However, the errors are large, as if we look at the hourly mean graphics, figure 19, we see that the smaller values of concentration for the day are around the 20 μg/m^3, which is larger than the smallest error of the table 17. Then, we can conclude that, during the weekdays, the best scheme is MYJ, although it does not give us an accurate prediction. As the PM_{10} are made of thousands of different particles, is hard to achieve an accurate model for them.

In order to see if the schemes represent the observed daily behavior of the PM_{10}, we will study the results of the stations of Sant Just Desvern (CEIP Montseny) and Barcelona (Parc Vall Hebron), the one with the best and the one with the worst prediction (figure 19). In both stations, the results of the model have a calm behavior: they do not present neither abrupted peaks nor deep valleys, contrary to the real datastation of Sant Jusp Desvern (figure 19a). This station present a cahotic behavior around the predicted data, close enough between them to have the smallest error. Then, the conclusion is that the model have not represented the daily behavior, although the error is the smaller. In the case of Vall d'Hebron (figure 19b), the values for all the observed data are below of the predicted data. Even though, the daily behavior of the observed data is similar to the predicted data this time.

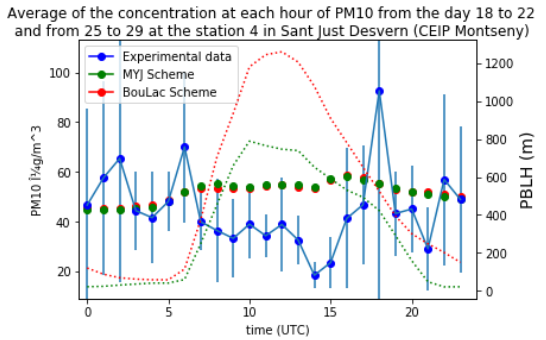

(a) Hourly mean using the model outputs of the weekdays for Sant Just Desvern (CEIP Montseny) station.

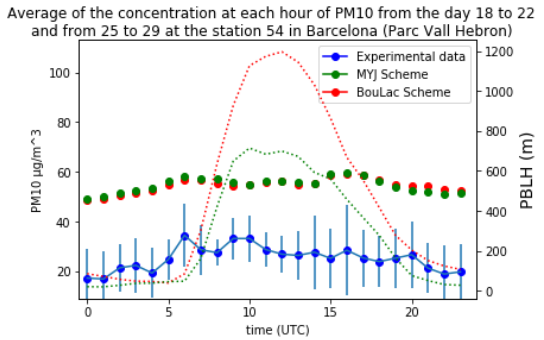

(b) Hourly mean using the model outputs of the weekdays for the Barcelona (Parc Vall Hebron) station.

Figure 19: The best and the worst predicted data for the PM_{10}.

We have seen that for the weekdays, the best scheme for the PM_{10} has been the MYJ. Then, looking for correlations between the best schemes and the characteristics of the stations is not neccesary. This time, the flashy fact for the PM_{10} is that we find significant differences modelling the weekdays and the weekends. If we look at the table 20, we observe now that there is 7 stations for the BouLac using the MBE and 6 using the RMSE! Fortunately for us, the differences of the errors are so light that we could choose the MYJ scheme at the weekend as well. This time, we will study the better shcemes for each stations comparing the map of the weekdays case with the weekend cases (figure 20). Moreover, in the table 19, we will look for the correlations among the best schemes and the characteristics of the station using the weekend data. We can see at the figure 20b, that the stations better predicted by the BouLac are those who are placed inside Barcelona and the urban area, whereas the MYJ works better at the periurban stations.

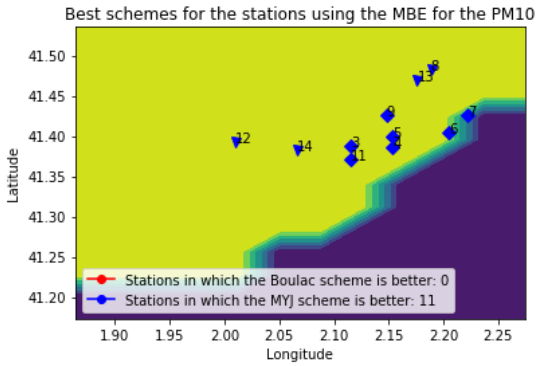

(a) Map of the metropolitan area of Barcelona showing the best scheme for each station using the MBE.

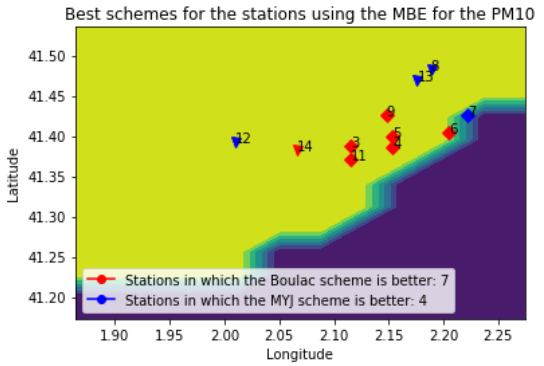

(b) Map of the metropolitan area of Barcelona showing the best scheme for each station using the RMSE.

Figure 20: Map placing the stations with the best scheme for each one for the PM_{10}. We can see the cities in the table 18. The $\diamond$ is for urban zones, $\triangledown$ for the periurban and the o for the rural. For the stations 1, 2 and 10, the data was not collected, for that reason they do not appear here.

City (station)	**MBE BouLac/MBE MYJ (scheme) ($\mu g/m^3$)**	**RMSE BouLac/ RMSE MYJ (scheme) ($\mu g/m^3$)**
Sant Just Desvern (CEIP Montseny)	7.151 / 7.164 (BouLac)	18.228 / 18.490 (BouLac)
Barcelona (Poblenou)	12.556 / 13.199 (BouLac)	16.045 / 15.986 (MYJ)
Sant Adria de Besos	16.492 / 16.321 (MYJ)	17.618 / 17.135 (MYJ)
Montcada i Reixac	16.981 / 16.594 (MYJ)	22.874 / 22.295 (MYJ)
Sant Vicenc dels Horts (Ribot)	18.964 / 18.457 (MYJ)	22.358 / 21.806 (MYJ)
Barcelona (Eixample)	19.467 / 20.425 (BouLac)	21.376 / 21.977 (BouLac)
Barcelona (Gracia - Sant Gervasi)	24.439 / 25.843 (BouLac)	25.118 / 26.345 (BouLac)
Hospitalet de Llobregat	24.946 / 25.850 (BouLac)	25.175 / 26.002 (BouLac)
Barcelona (Palau Reial)	27.369 / 28.273 (BouLac)	27.818 / 28.607 (BouLac)
Montcada i Reixac (Can Sant Joan)	29.092 / 28.779 (MYJ)	29.348 / 28.955 (MYJ)
Barcelona (Parc Vall Hebron)	29.464 / 29.666 (BouLac)	29.683 / 29.854 (BouLac)

Table 20: Table with the MBE and the RMSE for the comparison between BouLac and MYJ for the PM_{10} at the weekend.

Num	**City (station)**	**Num**	**City (station)**
3	Barcelona (Palau Reial)	9	Barcelona (Parc Vall Hebron)
4	Barcelona (Eixample)	11	Hospitalet de Llobregat
5	Barcelona (Gracia - Sant Gervasi)	12	Sant Vicenc dels Horts (Ribot)
6	Barcelona (Poblenou)	13	Montcada i Reixac (Can Sant Joan)
7	Sant Adria de Besos	14	Sant Just Desvern (CEIP Montseny)
8	Montcada i Reixac		

Table 18: Table referencing the stations in the figure 20.

	Zone		**Urban region**		
	Metropolitan Area	**Barcelona**	**Urban**	**Periurban**	**Rural**
MBE					
Proportion of stations (B/M)	2 / 4	5 / 0	6 / 1	1 / 3	0 / 0
RMSE					
Proportion of stations (B/M)	2 / 4	4 / 1	5 / 2	1 / 3	0 / 0

Table 19: Summary table for the map of the figure 20b for the PM_{10}.

The conclusion for the PM_{10} is that, even though both schemes present similar errors, the MYJ scheme is who better predicts the reality. Comparing the data given by the schemes with the real one, we realise that the error is still too large. The amount of different particles included in the PM_{10} does that this air pollutant is the one who present the biggest errors. We have seen that, for the weekend, the BouLac give us better results in the city of barcelona is the best schemes at urban regions. However, differences for the errors for MYJ and Boulac are really

close, then, we could use the MYJ scheme at the weekends without problem.

6 Conclusions

In that project, we have used the data of the "Xarxa de vigilància de la contaminació atmosfèrica", for the five air pollutants, in order to decide which PBL scheme represents better the contamitation of the Urban regions. Before anouncing the final decission, we will comment that we have observed how both schemes predict the expected behavior for the pollutants within the PBL, although we did not have general information for the behavior of the PM_{10}. We have seen that the most crowded stations with traffic,(the ones inside Barcelona), present larger errors compared to the the ones that are in the periurban zones. This fact is due to the emissions of each station.

The final decision is different depending on the air pollutants and the urban zone of the stations. For the CO, the ozone and the PM_{10}, the best scheme has been clearly the MYJ, although we can not extract conclusions for the ozone inside Barcelona. The reason is that the results for both schemes are too similar for the ozone there.

For the nitrogen oxides, the BouLac gains strength when we model stations inside Barcelona city. For the NO, we can affirm that the MYJ is the best scheme for modelling periurban stations, whereas we can not extract this conclusion for the NO_2.

In exception of the O_3, the best stations of each air pollutant present a really small error. These stations coincide with the periurban stations. This means that we are capable of simulating with exactitude some uncrowded regions! Another conclusion is that for the CO and the PM_{10}, we obtained results with shorter error for the weekends than for the weekdays.

References

[1] *Air pollution sources — European Environment Agency.* URL: https://www.eea.europa.eu/themes/air/air-pollution-sources-1.

[2] *Artículo : Principales contaminantes atmosféricos - Portal de Medio Ambiente.* URL: http://movil.asturias.es/portal/site/medioambiente/menuitem.1340904a2df84e62fe47421ca6108a0c/?vgnextoid=daca2ae109539210VgnVCM10000097030a0aRCRD&vgnextchannel=761ab1cc11b6a110VgnVCM1(i18n.http.lang=es.

[3] Alba Badia et al. "Description and evaluation of the Multiscale Online Nonhydrostatic AtmospheRe CHemistry model (NMMB-MONARCH) version 1.0: Gas-phase chemistry at global scale". In: *Geoscientific Model Development* 10.2 (2017). ISSN: 19919603. DOI: 10.5194/gmd-10-609-2017.

[4] P. Bougeault and P. Lacarrere. "Parameterization of orography-induced turbulence in a mesobeta-scale model". In: *Monthly Weather Review* 117.8 (1989). ISSN: 00270644. DOI: 10.1175/1520-0493(1989)117<1872:POOITI>2.0.CO;2.

[5] Fei Chen et al. "The integrated WRF/urban modelling system: Development, evaluation, and applications to urban environmental problems". In: *International Journal of Climatology* 31.2 (2011). ISSN: 08998418. DOI: 10.1002/joc.2158.

[6] L. K. Emmons et al. "Description and evaluation of the Model for Ozone and Related chemical Tracers, version 4 (MOZART-4)". In: *Geoscientific Model Development* 3.1 (2010). ISSN: 19919603. DOI: 10.5194/gmd-3-43-2010.

[7] *Foreword This User's Guide describes the Advanced Research WRF (ARW) Version 2.2 modeling system*. Tech. rep. URL: http://www.mmm.ucar.edu/wrf/users/..

[8] Georg Grell et al. "Fully coupled "online" chemistry in the WRF model". In: *Atmospheric Environment* 39 (Sept. 2005), pp. 6957–6975. DOI: 10.1016/j.atmosenv.2005.04.027.

[9] *Ground-level Ozone Basics — Ground-level Ozone Pollution — US EPA*. URL: https://www.epa.gov/ground-level-ozone-pollution/ground-level-ozone-basics.

[10] A. Guenther et al. "Estimates of global terrestrial isoprene emissions using MEGAN (Model of Emissions of Gases and Aerosols from Nature)". In: *Atmospheric Chemistry and Physics* 6.11 (2006). ISSN: 16807324. DOI: 10.5194/acp-6-3181-2006.

[11] Marc Guevara et al. "HERMESv3, a stand-alone multi-scale atmospheric emission modelling framework-Part 1: Global and regional module". In: *Geoscientific Model Development* 12.5 (2019). ISSN: 19919603. DOI: 10.5194/gmd-12-1885-2019.

[12] *Health Effects Carbon Monoxide Poisoning Exposure and Risk - CDC Tracking Network*. URL: https://ephtracking.cdc.gov/showCoRisk.action.

[13] Teddy Holt and Sethu Raman. *A review and comparative evaluation of multilevel boundary layer parameterizations for first-order and turbulent kinetic energy closure schemes*. 1988. DOI: 10.1029/RG026i004p00761.

[14] Xiao-Ming Hu, John W Nielsen-Gammon, and Fuqing Zhang. "Evaluation of Three Planetary Boundary Layer Schemes in the WRF Model". In: *Journal of Applied Meteorology and Climatology* 49.9 (Sept. 2010), pp. 1831–1844. ISSN: 1558-8424. DOI: 10.1175/2010JAMC2432.1. URL: https://doi.org/10.1175/2010JAMC2432.1.

[15] Z Janjic. "Nonsingular Implementation of the Mellor-Yamada Level 2.5 Scheme in the NCEP Meso model". In: *NCEP Office Note* 437 (2002).

[16] J. J. P. Kuenen et al. "TNO-MACC_II emission inventory: a multi-year (2003–2009) consistent high-resolution European emission inventory for air quality modelling". In: *Atmospheric Chemistry and Physics Discussions* 14.5 (2014). ISSN: 1680-7375. DOI: 10.5194/acpd-14-5837-2014.

[17] Shuyan Liu and Xin Zhong Liang. "Observed diurnal cycle climatology of planetary boundary layer height". In: *Journal of Climate* 23.21 (2010). ISSN: 08948755. DOI: 10.1175/2010JCLI3552.1.

[18] Alberto Martilli, Alain Clappier, and Mathias W. Rotach. "An urban surface exchange parameterisation for mesoscale models". In: *Boundary-Layer Meteorology* 104.2 (2002). ISSN: 00068314. DOI: 10.1023/A:1016099921195.

[19] Chin-Hoh Moeng. *Lecture Notes on The Planetary Boundary Layer*. Tech. rep. URL: http://library.ucar.edu/research/publish-technote.

[20] *Nitrogen Oxides: Your Environment, Your Health — National Library of Medicine*. URL: https://toxtown.nlm.nih.gov/chemicals-and-contaminants/nitrogen-oxides.

[21] *Ozone Pollution and its Impact on Climate and Health — CAG*. URL: https://www.cag.org.in/blogs/ozone-pollution-and-its-impact-climate-and-health.

[22] *Química estratosférica. La capa de ozono.* URL: https://www.ugr.es/~mota/Parte1-Tema01.pdf.

[23] Francisco Salamanca et al. "A new building energy model coupled with an urban canopy parameterization for urban climate simulations-part I. formulation, verification, and sensitivity analysis of the model". In: (Sept. 2010).

[24] I D Stewart and T Oke. "Local Climate Zones for Urban Temperature Studies". In: *Bulletin of the American Meteorological Society* 93 (Dec. 2012), pp. 1879–1900. DOI: 10.1175/BAMS-D-11-00019.1.

[25] R. B. Stull. "An introduction to boundary layer meteorology". In: *An introduction to boundary layer meteorology* (1988). DOI: 10.1007/978-94-009-3027-8.

[26] Xuexi Tie et al. "Effects of lightning on reactive nitrogen and nitrogen reservoir species in the troposphere". In: *Journal of Geophysical Research Atmospheres* 106.D3 (2001). ISSN: 01480227. DOI: 10.1029/2000JD900565.

[27] Xuexi Tie et al. "Global NOx production by lightning". In: *Journal of Atmospheric Chemistry* 43.1 (2002). ISSN: 01677764. DOI: 10.1023/A:1016145719608.

[28] Gerhard Wotawa, Paul Novelli, and C Granier. "Inter-annual variability of summertime CO concentrations in the Northern Hemisphere explained by boreal forest fires in North America and Russia". In: *Geophysical Research Letters - GEOPHYS RES LETT* 28 (Sept. 2001), pp. 4575–4578. DOI: 10.1029/2001GL013686.